A NUCLEAR MAGNETIC RESONANCE SPECTROMETER

A NUCLEAR MAGNETIC RESONANCE SPECTROMETER

By

KENNETH ARTHUR LINES, B.Sc.

A Thesis

Submitted in Partial Fulfilment of

the Requirements for the Degree

Master of Science in the

Department of Physics

McMaster University

McMaster University

September 1955

Acknowledgments

The author wishes to acknowledg the encouragement of Dr. H. E. Petch under whose direction this work was accomplished. He is indebted to Mr. F. Holuj who constructed one of the pieces of apparatus, the d.c. amplifier, and who supplied a sodium dihydrogen phosphate crystal. The Defense Research Board made this work possible through its financial support. The Consolidated Mining and Smelting Company, Trail, British Columbia, through its fellowship enabled the author to continue his studies.

Contents

A Nuclear Magnetic Resonance Spectrometer

Introduction

The magnetic properties of the nucleus have interested Physicists ever since they were first postulated to explain the hyperfine structure of spectral lines. It was supposed that the nucleus is, in general, a small magnet whose interaction with the atomic electron splits the energy levels between which the electron make transitions responsible for atomic linespectra. With spectroscopic instruments of high resolving power it was possible to determine certain nuclear spins and to measure a number of nuclear magnetic moments to about two significant figures (1). Considerably more accurate measurements were obtained in molecular beam measurements (2)(3) which were pioneered under O. Stern and which later flourished under Rabi at Columbia University. An outstanding addition to the beam techniques was the magnetic resonance method which the Rabi group applied to these experiments. In the most recent developements in the study of nuclear magnetic moments, the magnetic resonance principle has been applied to solids, liquids and gases in their normal physical states and in consequence the compilation of data concerning nuclear magnetism has become even more rapid.

These new magnetic resonance techniques were developed simultaneously and independently by the Purcell and Pound group(4)(5) at Harvard and the Bloch and Hanson group(6)(7) at Stanford. The advantages of the new magnetic resonance method over other methods

are the relatively simpler equipment, greater accuracy and wider applicability.The magnetic moments of most of the stable nuclei have now been measured. However, as a result of the interaction between a nucleus and its surroundings this method can be used as a tool to study other effects. For example it has been used to study the establishment of the thermal equilibrium essential to magnetic methods for attaining very low temperatures. The width and shape of the resonance has yielded information concerning crystal structure, (8)(9), phase transitions in solids (10) and hindered internal motions in solids (11).

Theory

(1) Nuclear Angular Momentum

The angular momentum of any particle or system of particles is found to be easily expressed in terms of a fundamental unit $\frac{h}{2\pi}$ which is Plancks constant divided by 2π. The quantity denoted as "the spin" is defined as $\frac{1}{\frac{h}{2\pi}}$ times the largest observable value of the time average of a component of the angular momentum vector $\overline{p}$ in a given direction. Since we are concerned with magnetic fields we shall select the direction of an applied magnetic field H as the reference direction of interest to us. From quantum-mechanical arguments the value of the vector $\overline{p}$ is

$$|\overline{p}| = \left[I(I+1)\right]^{\frac{1}{2}} \frac{h}{2\pi} \qquad (1)$$

where I is the quantity refered to as "the spin quantum number"

$$I = \left(\frac{1}{\frac{h}{2\pi}}\right)(p_H)_{max} \qquad (2)$$

and p_H is given by the expression

$$p_H = m\frac{h}{2\pi}$$

where m = I, I-1, $\cdots$ -I+1, -I

It is found experimently and theoretically that the value I can only take integral or half integral values so that the angular momentum is limited to discrete values.

(2) Nuclear Magnetic Moment

In addition to its intrinsic angular momentum a nucleus possesses, in general, a magnetic moment; that is it acts like a

small bar magnet. This magnetism may be considered to originate is circulating currents in the nucleus. Since the intrinsic angular momentum implies a circulation of mass, it should not be surprising if the angular momentum and magnetic moment are related. From classical mechanics, the magnetic moment of a spinning spherical shell with charge q and mass m distributed uniformly over the surface is

$$\overline{\mu} = \left(\frac{e}{2mc}\right) \overline{p} \tag{4}$$

where $\overline{\mu}$ is the magnetic moment, $\overline{p}$ is the angular momentum and c is a constant equal to the velocity of light in free space. Since nuclear magnets do not conform to this simple model it is customary to write

$$\overline{\mu} = g \left(\frac{e}{2Mc}\right) \overline{p} \tag{5}$$

where g , called the nuclear g factor, is a number characteristic of a nuclear species in a given energy state, · is the charge on a proton and M is the mass of a proton.

Equation (5) can also be written

$$\overline{\mu} = g \left(\frac{e}{2Mc}\right) \frac{h}{2\pi} \overline{I} = g u_o \overline{I} \tag{6}$$

where $u_o = \frac{e}{2Mc} \frac{h}{2\pi}$ is called the nuclear magneton. Nuclear magnetic moments are usually given in terms of the nuclear magneton. The quantity colloquially refered to as "the magnetic moment" is

$$(u_H)_{max} = gIu_o \tag{7}$$

The dimensionless number gI is "the magnetic moment" measured in units of the nuclear magneton.

(3) Nuclear Electric Quadrupole Moment

In addition to intrinsic angular momentum and a magnetic moment a nucleus may also possess an electric moment. If one expands the electrostatic potential at a point outside the nucleus in terms of an infinite series, one finds that the successive terms correspond to higher and higher order electric"momenta". The first term of the expansion represents the potential of a monopole. Since this term is spherically symmetric, the electrostatic energy due to this monopole is independent of nuclear orientation. Therefore this term is of no further interest in this work. The second term of the expansion is called the dipole moment. However, the theory of nuclear structure says that this term is zero(12), so it need not be considered further. The third term is the quadrupole moment. This moment is a measure of the departure from spherical symmetry of the nuclear charge distribution. The electric quadrupole moment of the nucleus can be either positive or negative, the positive value indicating an oblate spheroid with respect to the nuclear spin axis. A negative value indicating a prolate distribution of charge. For a nucleus to have a quadrupole moment the spin I must be greater than or equal to 1 (13). The nuclear quadrupole moment is defined as

$$e\,Q = \iiint \rho(z^2 - r^2)\,dv \qquad (8)$$

where e is the proton charge, ρ is the charge density on the nucleus. Because of the nuclear symmetry it turns out that the nuclear quadrupole moment is a scalar quantity. The higher order terms are in general negligible and shall not be considered here

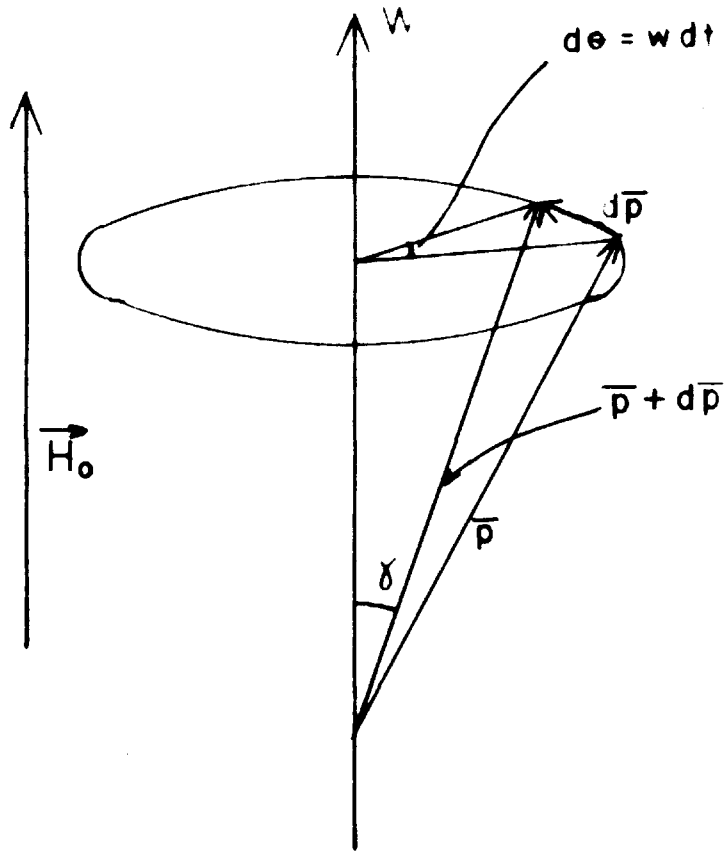

FIG.(1) VECTOR DIAGRAM USED TO ILLUSTRATE THE DIFFERENTIAL EQUATION OBEYED BY A PRECESSING ANGULAR MOMENTUM VECTOR OF CONSTANT MAGNITUDE

(4) Interaction of a Nuclear Magnetic Moment with an Applied Magnetic Field

If a magnet of dipole moment $\bar{\mu}$ is placed in a magnetic field $\bar{H}_o$, a torque $\bar{L}$ is exerted on this magnetic dipole

$$\bar{L} = \bar{u} \times \bar{H}_o \tag{9}$$

Newtons law of rotational motion states that the rate of change of angular momentum is equal to the torque applied to it

$$\frac{d\bar{p}}{dt} = \bar{L} \tag{10}$$
$$\therefore \frac{d\bar{p}}{dt} = \bar{u} \times \bar{H}_o$$

since $\bar{\mu} = g \left(\frac{e}{2Mc}\right) \bar{p}$

$$\frac{d\bar{p}}{dt} = -g \left(\frac{e}{2Mc}\right) \bar{H}_o \times \bar{p} \tag{11}$$

which is the equation of motion for a vector p of constant magnitude precessing with angular velocity

$$\bar{\omega}_o = -g \left(\frac{e}{2Mc}\right) \bar{H}_o \tag{12}$$

We see that if a nucleus with magnetic moment u is placed in a magnetic field $\bar{H}_o$ the angular momentum vector $\bar{p}$ precesses with angular frequency $\bar{\omega}_o$ regardless of the angle γ between $\bar{u}$ and $\bar{H}_o$. $\bar{\omega}_o$ is called the Larmor precession frequency.

Although the Larmor precession frequency remains constant it can be shown that the potential energy of the nuclear dipole is a function of the angle γ between $\bar{\mu}$ and $\bar{H}_o$.

As we have shown earlier the nuclear dipole make only certain definite angles with H_o. Therefore, there will be only discrete values of potential energy available to the dipole.

The potential energy U of a magnetic dipole of moment $\bar{\mu}$ in a magnetic field $\bar{H}_o$, apart from an additive constant, is

$$U = -\bar{\mu} \cdot \bar{H}_o = -u_H \cdot H_o \tag{13}$$

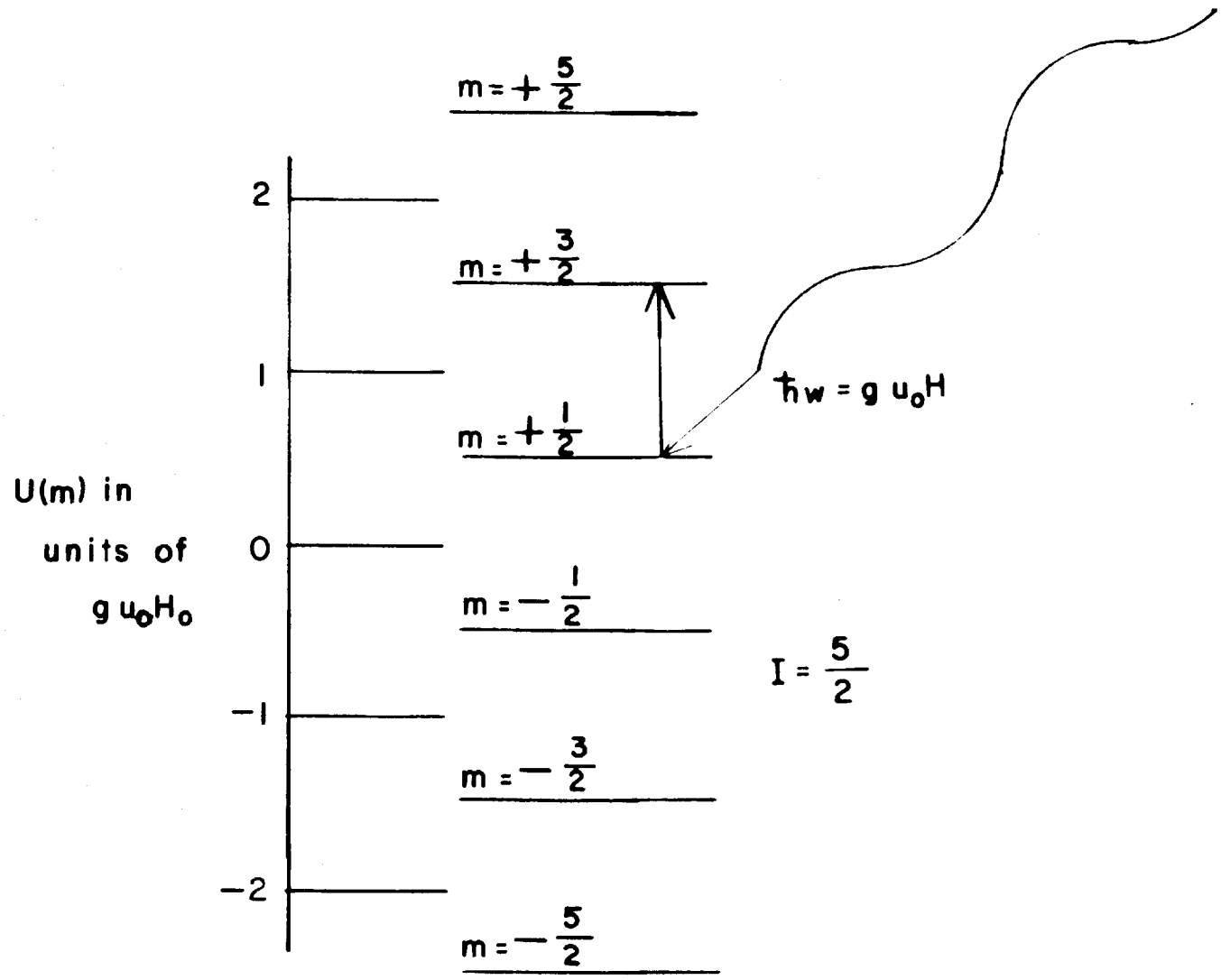

FIG.(2) ENERGY LEVEL DIAGRAM FOR A [illegible]
WITH A NEGATIVE MAGNETIC MOMENT AND SPIN I = 5/2
SHOWING SCHEMATICALLY THE ABSORPTION OF A
QUANTUM OF RADIATION WHICH INDUCES A
TRANSITION BETWEEN A PAIR OF ADJACENT [illegible]
BANDS SPLIT BY A MAGNETIC FIELD.

If a nucleus is in a state m this energy will be

$$U_m = -g \left(\frac{e}{2Mc}\right) mH \qquad (14)$$

Since m can take the values m = I, I-1, ··· -I a nucleus in a magnetic field has 2I+1 energy levels accessible to it.

(5) Absorption of Energy

It has been shown in the previous section that a nuclear dipole in a purely magnetic field has 2I+1 energy levels accessible to it by virtue of its interaction with that field. The energy difference between two such levels is given by

$$\Delta U = U(m'') - U(m') = g u_o H_o (m' - m'') \qquad (15)$$

It is apparent that the energy levels must be evenly spaced. Transitions are possible between these energy levels providing the selection rule $\Delta m = \pm 1$ is satisfied. Such a transition is accompanied by either absorption of emission of a quantum of radiation of energy

$$h\omega = \Delta U \qquad (16)$$

Substituting equation (15) for the case $\Delta m = -1$ into (16) gives as the frequency for the radiation absorbed or emitted

$$\omega_o = -g \left(\frac{e}{2Mc}\right) H_o$$

which is precisely the Larmor precession frequency given by equation (12) Since $u_o = \left(\frac{eh}{2Mc}\right)$ equation (12) transforms into

$$\hbar\omega_o = g u_o H_o \qquad (17)$$

From equation (6) we get the result

$$h\nu_o = \frac{u H_o}{I} \qquad (18)$$

For protons in a magnetic field of 10,000 gauss, $\nu_o = 42.6 \times 10^6$ sec^{-1} which is in the radio frequency range.

If one subjects a sample containing nuclear magnets to radiation of the Larmor frequency, which is of the order of a few megacycles/sec in ordinary laboratory fields, a nucleus in a lower energy state may absorb a quantum of energy and make a transition to the next higher energy state. If the frequency is not at the Larmor precession frequency no absorption will occur. This absorption is called the resonance phenomenon.

(6) Interaction of the Nuclear Electric Quadrupole Moment with an Electric Field Gradient.

It has been shown in section(1) that a nucleus of spin I and magnetic moment $\bar{\mu}$ placed in a constant uniform magnetic field $\bar{H}_o$ has 2I 1 Zeeman levels with a constant energy difference $h\nu_c = uH_o/I$ The 2I transitions between adjacent levels ($\Delta m = \pm 1$) all correspond to a single resonance frequency ν_c, giving rise to a single absorption line.

If the nucleus in question has $I > \frac{1}{2}$ it may also have an electric quadrupole moment which can interact with an electric field gradient, caused by a non-spherical charge distribution outside the nucleus, to produce a dependence of the electrostatic energy of the system on nuclear orientation. Pound(14) has shown that the effect of this second interaction is that each of the Zeeman levels is shifted, and the single absorption line of frequency ν_o is split into 2I components. In the case that the quadrupole coupling energy is small compared to the magnetic coupling energy, Pound has shown that first order perturbation theory gives for the frequency of the transition between the perturbed Zeeman levels m and m-1 the value

$$\nu(m \leftrightarrow m-1) = \nu_o \mp \frac{3eQ(2m-1)}{4I(2I-1)h} \phi_{z'z'} \qquad (19)$$

where $\phi_{z'z'}$ is the second derivative of the electrostatic potential at the site of the nucleus in question, the z' direction coinciding with that of the constant magnetic field H_o and the sign is to be chosen opposite to the sign of the nuclear gyromagnetic ratio. It is easily seen from equation (19) that in this first order approximation the two resonance frequencies $\nu(m \leftrightarrow m-1)$ and $\nu(-(m-1) \leftrightarrow -m))$ lie equally spaced on opposite sides of ν_o, the frequency difference between them being given by twice their separation from the unperturbed line ν_o.

If the orientation of the crystal is varied with respect to the constant magnetic field H_o the value of $\phi_{z'z'}$ along H_o will vary, and the observed splitting will be a function of crystal orientation. Let eq denote the value of $\phi_{z'z'}$ for that particular crystal which gives the greatest splitting. The equation (19) may be written in the form

$$\nu(m \leftrightarrow m-1) = \nu_o \mp \frac{3(2m-1)}{4I(2I-1)} \frac{e^2qQ}{h} \frac{\phi_{z'z'}}{eq} \qquad (20)$$

Here the first factor depends on the spin I of the nucleus and on the particular components of the line being investigated, the second factor os the so-called quadrupole coupling constant, and the third dimensionless factor of absolut value not exceeding unity depends on the orientation of the crystal in the magnetic field.

The electric quadrupole interaction may be sufficiently strong that first order perturbation theory is inadequate, and second order perturbation theory must be used. The expression for the frequency shift when it is necessary to consider the perturbation to the second order, will not be reproduced here. However, although the expression

is much more complicated than the first order result, it is similar in that it contains a number of terms involving the spin and particular components of the line being investigated, the quadrupole coupling constant and factors which depend on the orientation of the crystal in the magnetic field. Second order theory predicts that the central linewill also shift in frequency.

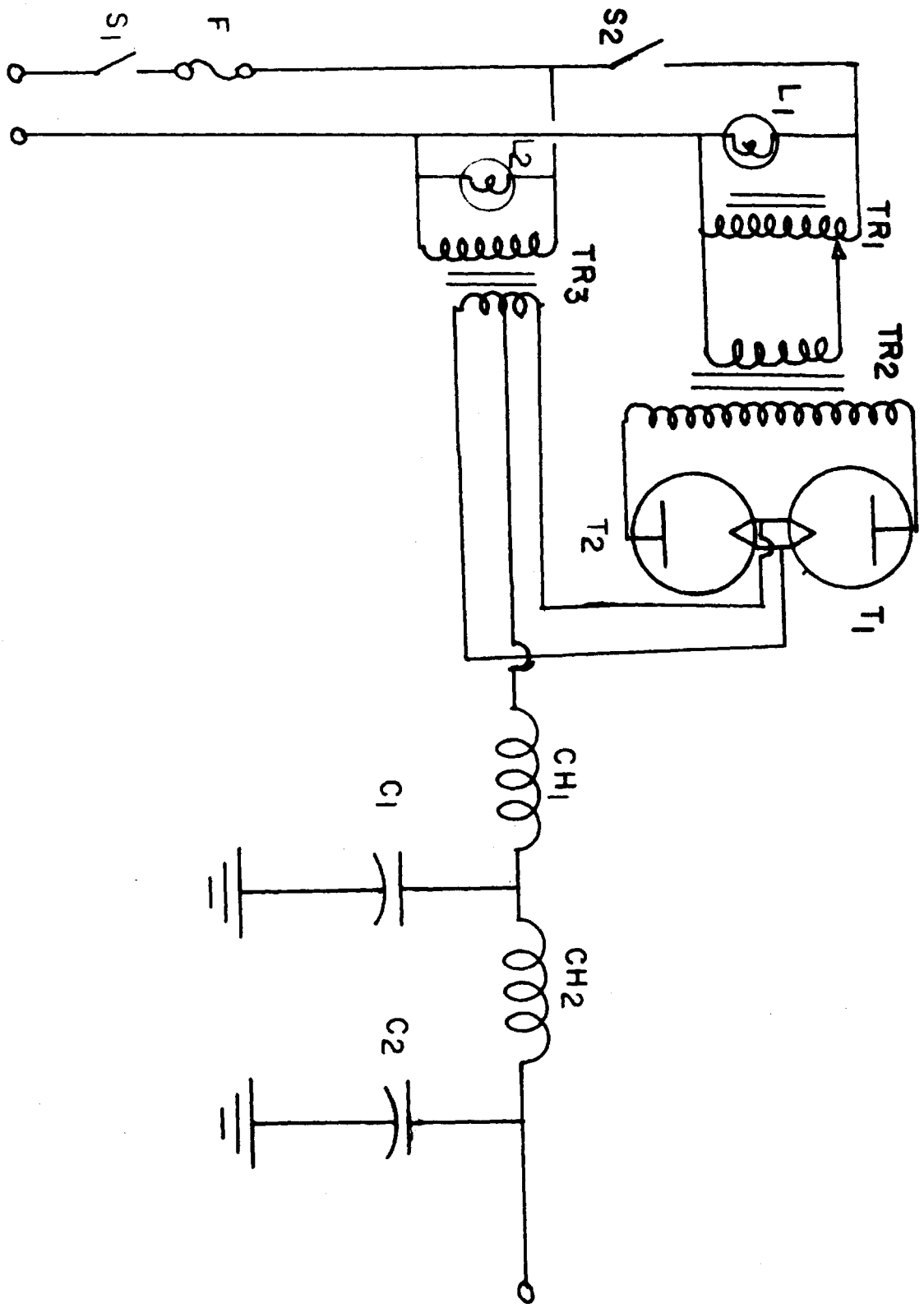

Fig (3

Apparatus

(1) Magnet

The most essential piece of apparatus for nuclear magnetic resonance experiments is a large magnet capable of producing a highly uniform and highly stabilized magnetic field. A suitable electromagnet was salvaged from a discarded mass spectrometer. New pole pieces for the magnet were carefully ground in order to get a more uniform field and the gap was set at one inch.

The two coils for the magnet each consist of 20,000turns of #26 formex magnet wire. Sheet copper was wrapped aroun the magnet coils and copper tubing was soldered to the sheeting. Cold water was forced through the copper tubing and the resultant cooling made it possible to operate the magnet at slightly higher field strength without damage to the coils from overheating.

(2) Magnet Power Supply

An unstabilized magnet current supply was also salvaged from the discarded mass spectrometer. This is shown in figure (3). It consists of a 1,500 volt Hammond power transformer with a variac in the primary circuit to control the output. Full wave rectification is provided by two 866-A mercury vapor tubes and the d.c. output is smoothed by a special high voltage choke and high voltage condensers connected to make a π filter. It is capable of supplying approximately 500 ma at 1700 volts.

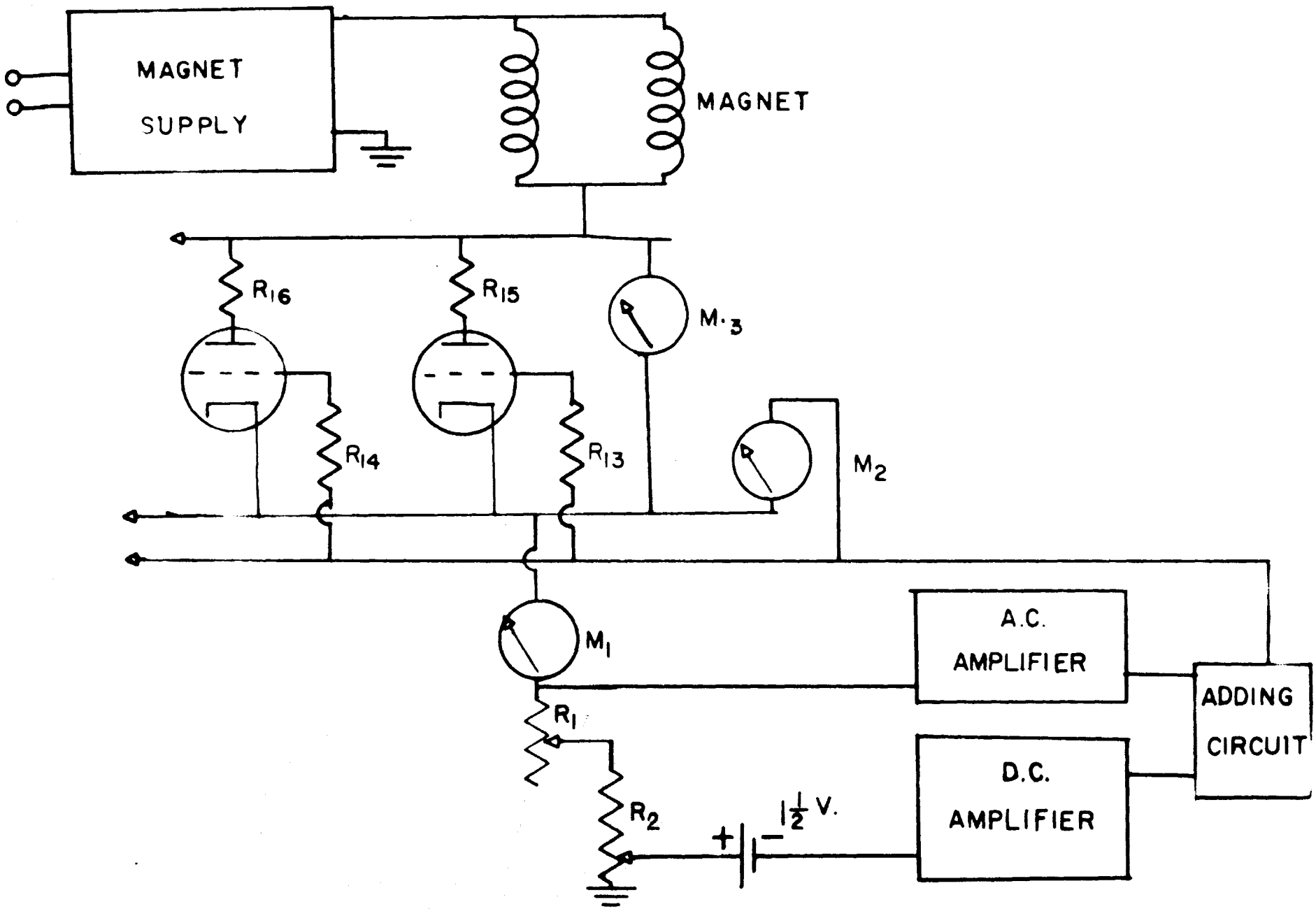
MAGNET
SUPPLY
MAGNET
R16
R15
M3
R14
R13
M2
M1
A.C.
AMPLIFIER
ADDING
CIRCUIT
R1
R2
½ V.
D.C.
AMPLIFIER

Fig. (4)

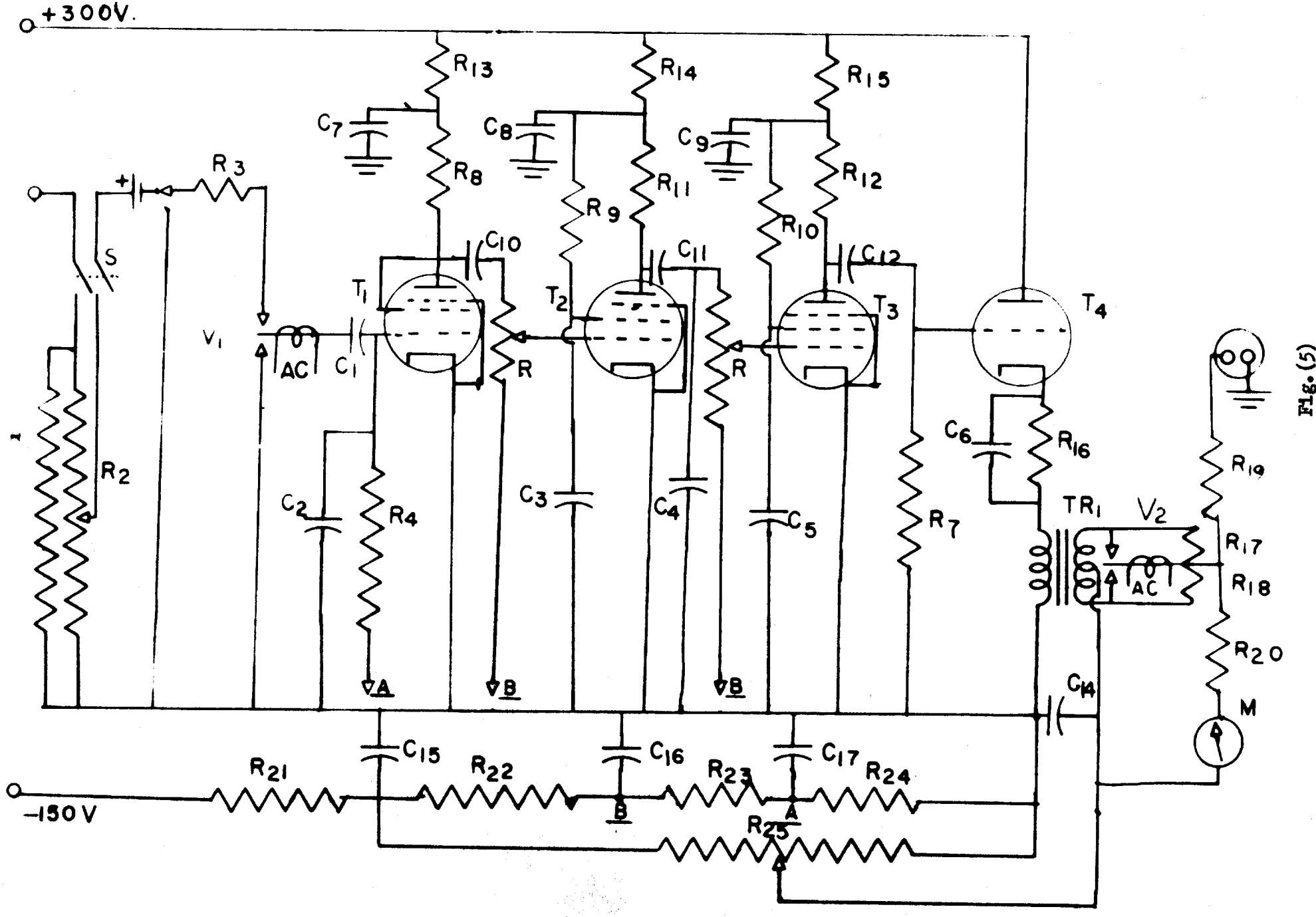
+300V.
R13
R14
R15
C7
C8
C9
R8
R9
R11
R10
R12
R3
S
C10
C11
C12
T1
T2
T3
T4
V1
AC
C1
R
R
R2
C2
R4
C3
C4
C5
R7
C6
R16
TR1
V2
R19
R17
R18
R20
M
C14
A
B
B
C15
C16
C17
R21
R22
R23
R24
R25
-150 V

Fig. (5)

(3) Stabilizing Circuit for the Magnet supply

(a) General Circuit

A block diagram of this circuit is shown in figure (4). It consists of five 6B4 series control tubes in parallel. D.C. and A.C. error amplifiers convert changes in the voltage across resistors R1 and R2 into error signals which are fed degeneratively onto the grids of the 6B4 control tubes. These signals are of the correct magnitude and phase to correct to a high degree any change in the magnet current.

(b) D.C. Amplifier

The conventional form of D.C. amplifier possesses certain disadvantages. Since the grid of any tube is connected directly to the plate of the preceding tube, the number of tubes in the circuit is severely limited. The amplification is also limited due to the danger of cutting the last tube off with large swings of potential. Also since the characteristics of radio tubes change with time, serious drifting is caused in the amplified signals.

Since these disadvantages are absent in an A.C. amplifier, this type of amplifier is used in this circuit. It converts the D.C. error into an A.C. signal, amplifies it and converts it back to a D.C. correction signal. This circuit is shown in figure (5). The magnet current passes through the resistors R1 and R2. A flashlight battery is connected in the circuit in such a way as to oppose the potential from the tap on R2 so that when the correct current is flowing the potential at the chopper V1 is zero. If the current change slightly

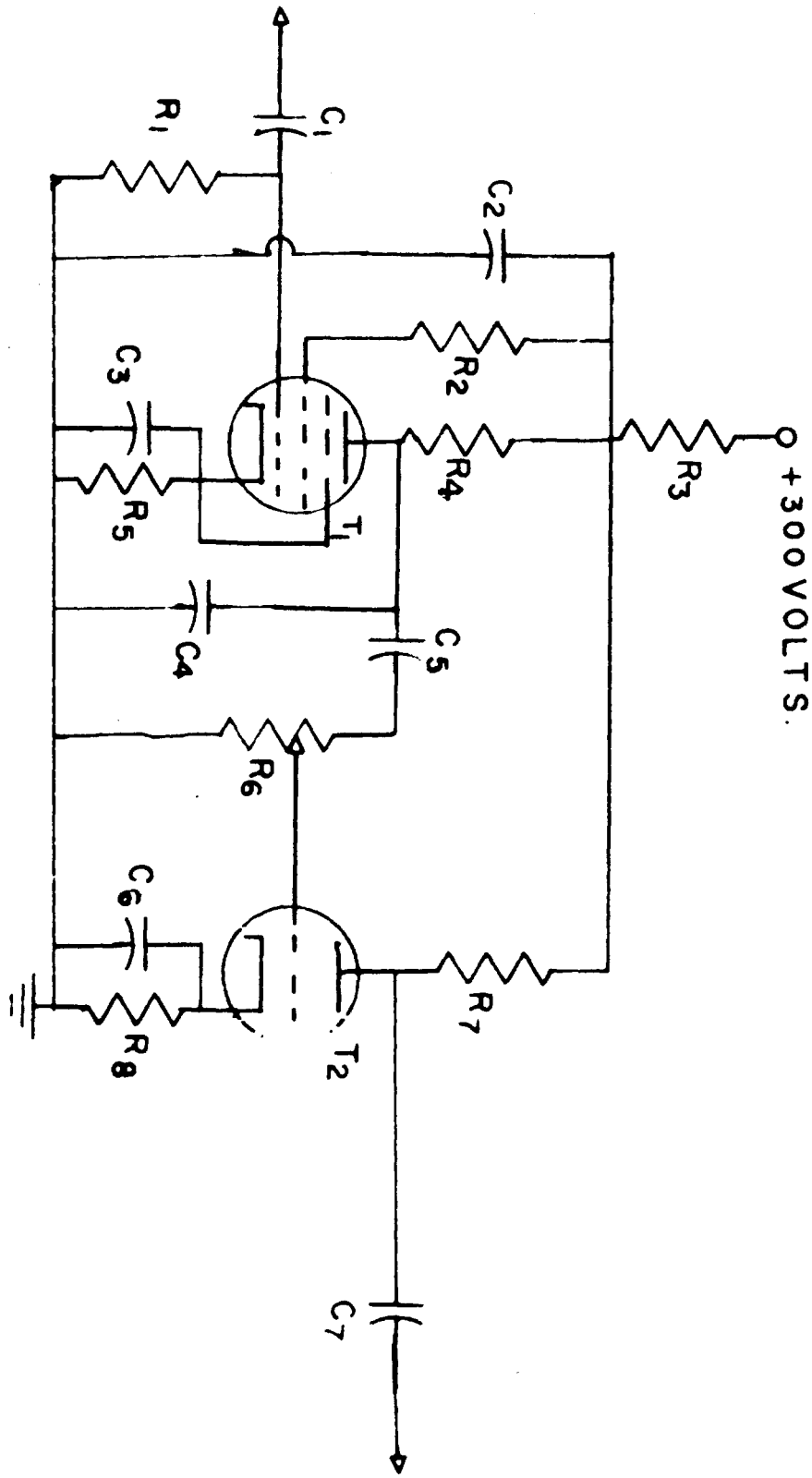

Fig. (6)

the potential at V1 becomes different from zero. The chopper V1 converts this D.C. potential to a 60cycle/sec square wave which is amplified in the following three stage amplifier. The amplitude of the 60cycle/sec square wave signal is proportional to the error in the current. The amplified square wave is converted into a D.C. error signal by a second chopper V2, which is connected so that it operates as a phase sensitive rectifier. The filtered D.C. error signal is fed through the adding circuit (fig.4) onto the grids of the series control tubes (T6 and T7). This changes the magnet current which flows through the series control tubes, which then makes the potential at V1(fig.5) return to zero. A ten turn Helipot R2 is used to obtain fine adjustment of the magnet current. Condensers C2 and C4 are added to eliminate high frequency spikes on the square waves. They affect very little the shape and phase of the square waves.

(c) A.C. Amplifier.

Since the choppers operate at 60cycles/sec, the D.C. amplifier will only respond to dhange of the order of a thirtieth of a second. To compensate for rapid changes and random pulses in the magnet current an A.C. amplifier was built. This is shown in figure (6) This is seen to be a simple two stage amplifier and needs no further description.

(d) Adding Circuit

The output from the two amplifiers just described are fed into an adding circuit shown in figure (7). Cathode followers are used

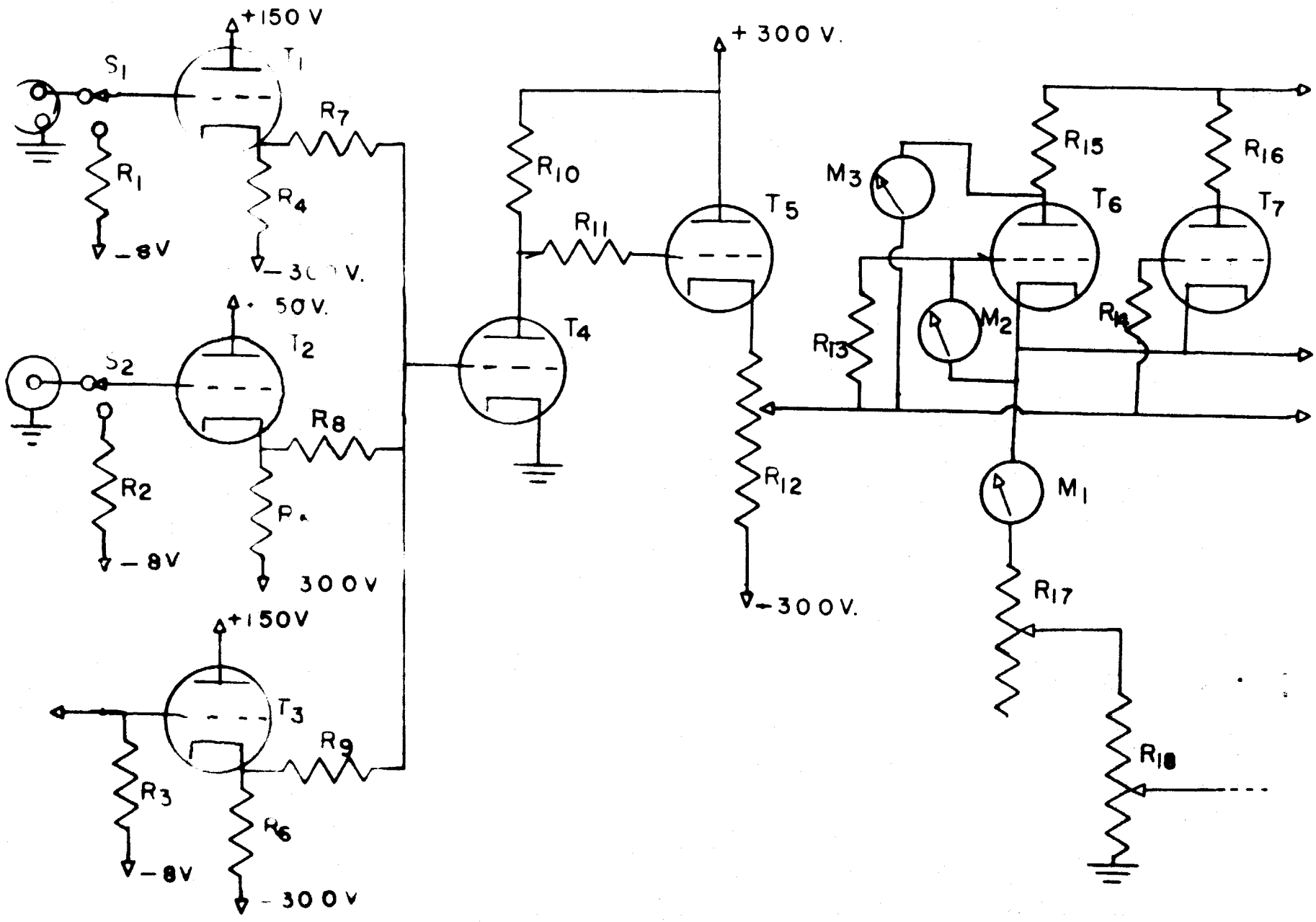
+150 V
S1
T1
R7
R1
R4
-8V
-300 V.
+ 50V.
T2
S2
R8
R2
P
-8V
300 V
+150V
T3
R9
R3
R6
-8V
-300 V
+ 300 V.
R10
R11
T5
T4
R12
-300 V.
M3
R15
R16
T6
T7
R13
M2
R14
M1
R17
R18

Fig. (7)

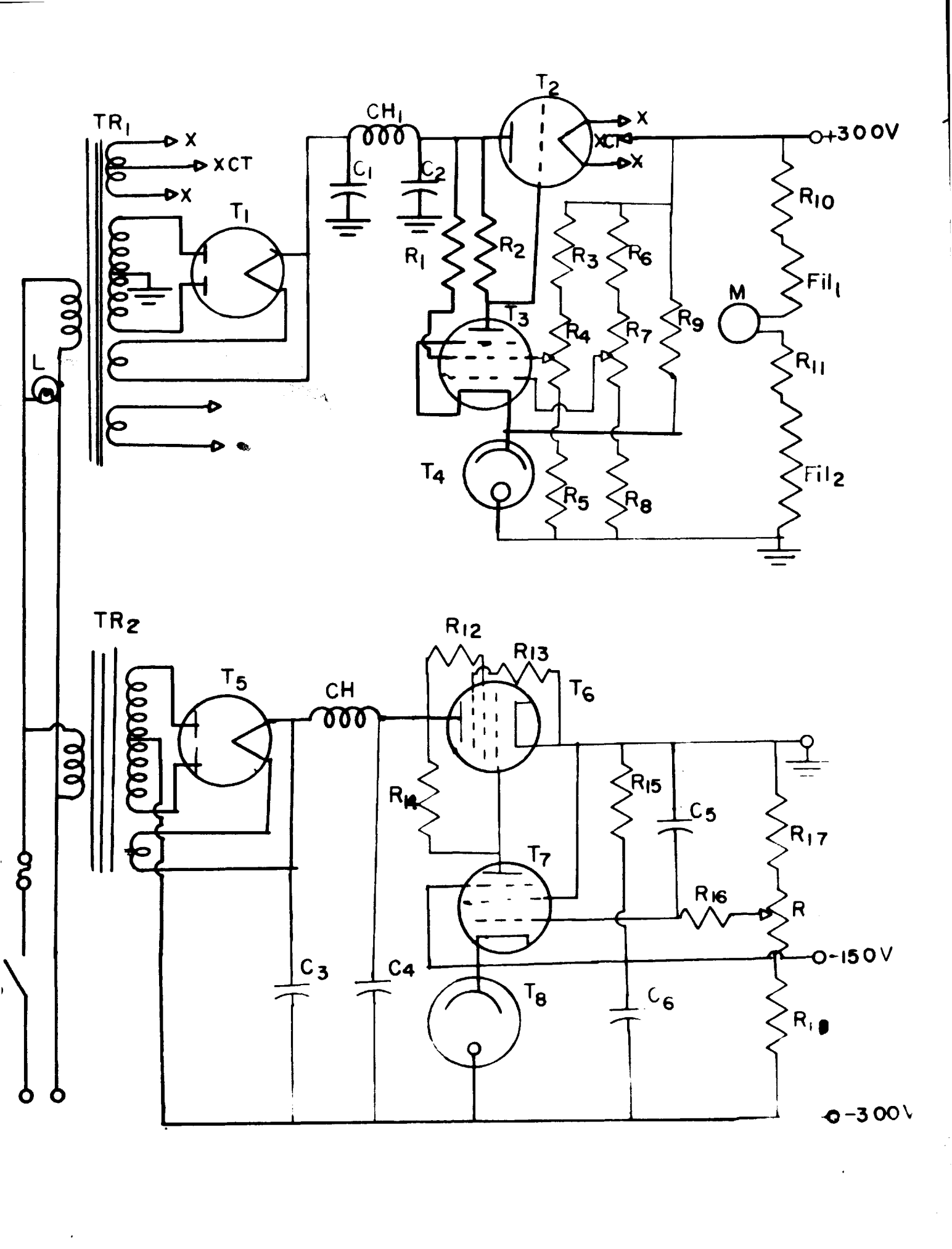
TR1
X
XCT
X
T1
CH1
C1
C2
R1
R2
T2
X
XCT
X
+300V
R10
Fil1
M
R11
Fil2
T3
R3
R6
R4
R7
R9
T4
R5
R8
L
TR2
T5
CH
R12
R13
T6
R14
R15
C5
R17
T7
R16
R
-150V
C3
C4
T8
C6
R18
-300V

to couple the amplifiers to the adding stage because of their good decoupling properties in the reverse direction. The error signals are added together at the grid of tube T_4, and the composite signal is amplified and fed to the series control tubes through a cathode follower T5. This cathode follower is connected between + 300 and -300 Volts in order to provide a wide range of potential available for large correction signals. Grid stopping resistors are used in the five series control tubes to reduce any tendency for oscillations to start. Small value resistors are used in the plates of the control tubes to to equalize the current through the tubes. T_2 is an extra input tube which is not being used at present buthas been built in for future use with proton stabilization.

(e) Stabilized Power Supply for the Error Amplifiers and Adding Circuit

This supply is shown in figure(8). It consists of two separate supplies mounted on the same chasis, one supply giving + 300 volts the other -300 volts. Both of these supplies are of the degenerative type The comparison voltage is provided by the VR 150(T4 and T8) tubes, connected to the stabilized side of the supply. Part of the screen potential of pentode T_3 comes from the unregulated side of the supply. This part may be regarded as a small forward acting component of the screen potential which effectively increases the stabilization ratio to a large degree. Any ripple component which is sinusoidal can be easily eliminated this way. The connection of plate load resistors to the unstabilized side of the supply is no disadvantage for a

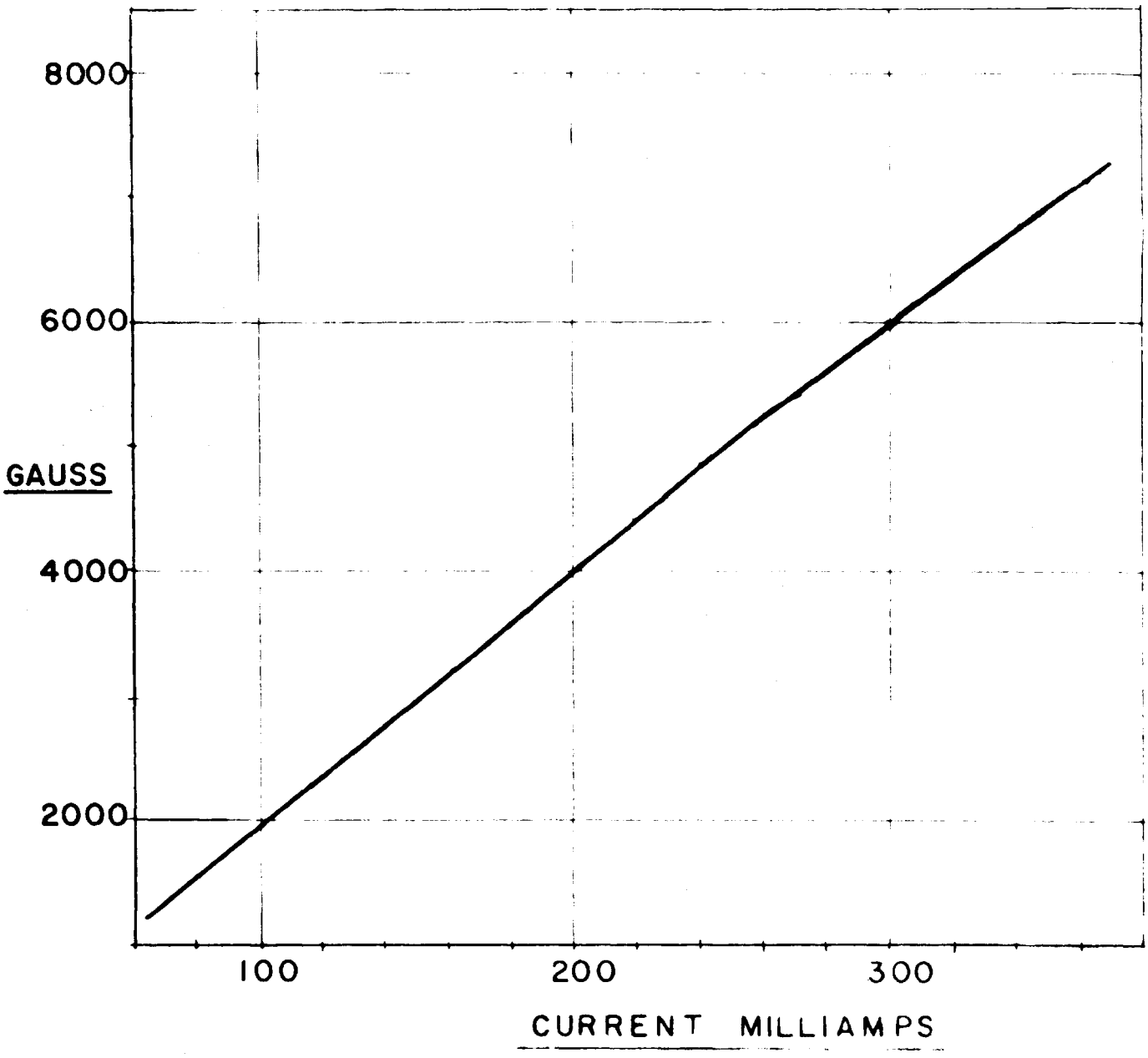

MAGNET FIELD-CURRENT CALIBRATION

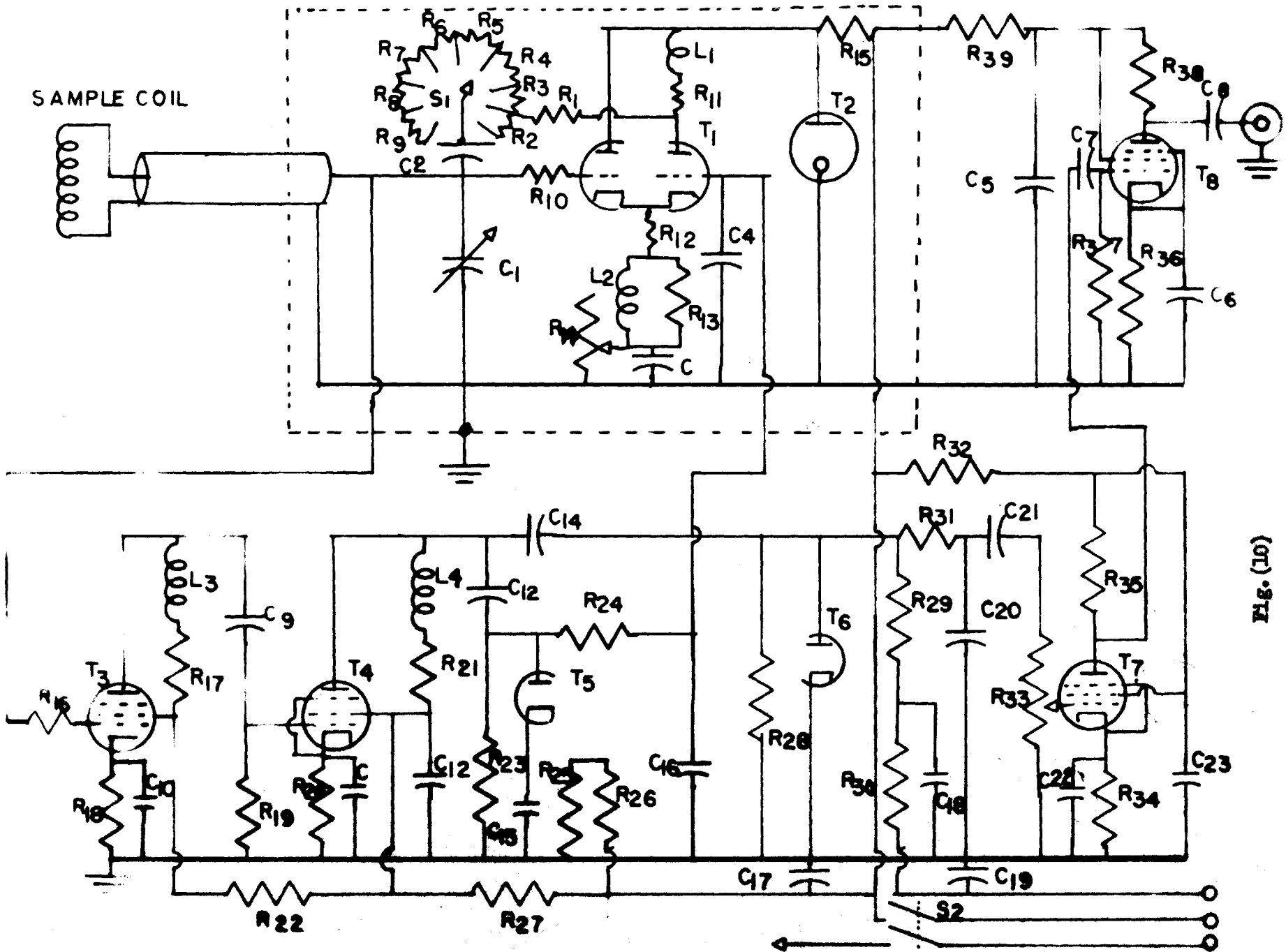
SAMPLE COIL
R6
R5
R7
R4
R8
S1
R3
R1
R9
R2
C2
L1
R11
T1
R10
R12
C4
C1
L2
R13
C
R15
T2
R39
R38
C8
C7
T8
C5
R37
R36
C6
R32
C14
R31
C21
L3
C9
L4
C12
R24
T6
R29
C20
R35
T3
R17
T4
R21
T5
T7
R33
R16
R28
C12
R23
C16
R30
C18
C23
C10
R18
R19
C
R26
C15
C17
C19
R22
R27
S2

Fig. (10)

pentode, but instead improves the stabilization due to the larger range of voltage provided. The filament supply for the A. C. and D.C. amplifiers is direct current obtained from the 300 volts by 100 watt voltage dropping resistors.

(f) Magnet Field Current Calibration.

The graph giving the magnetic field for a given current passing through the coils in parallel, is shown in figure (9).

(4)(a) Oscillating Detector

The oscillating detector, figure (10) which has been built is of the Pound and Knight type (15) and consists essentially of a radio frequency coil in which the sample is placed. Both are then mounted in a strong uniform magnetic field with the axis of the coil perpendicular to the magnetic field. The radio frequency coil is connected by means of a coaxial cable parallel with a variable condenser to form a shunt resonant circuit.

Oscillations are just barely maintained in this resonant circuit by a cathode coupled oscillator, so that the r.f. level is very sensitive to power losses in the tank coil of the oscillator. The r.f. level is kept very low by the combination of a variable cathode bias and variable grid bias on T1. The sensitivity of the circuit is dependent on the level of oscillation and is most sensitive at the oscillation threshold.

The r.f. is amplified by a broad band r.f. amplifier(T3 and T4) and detected by two detector tubes(T5 and T6). The audio signal from the first detector T6 is further amplified by two audio stages

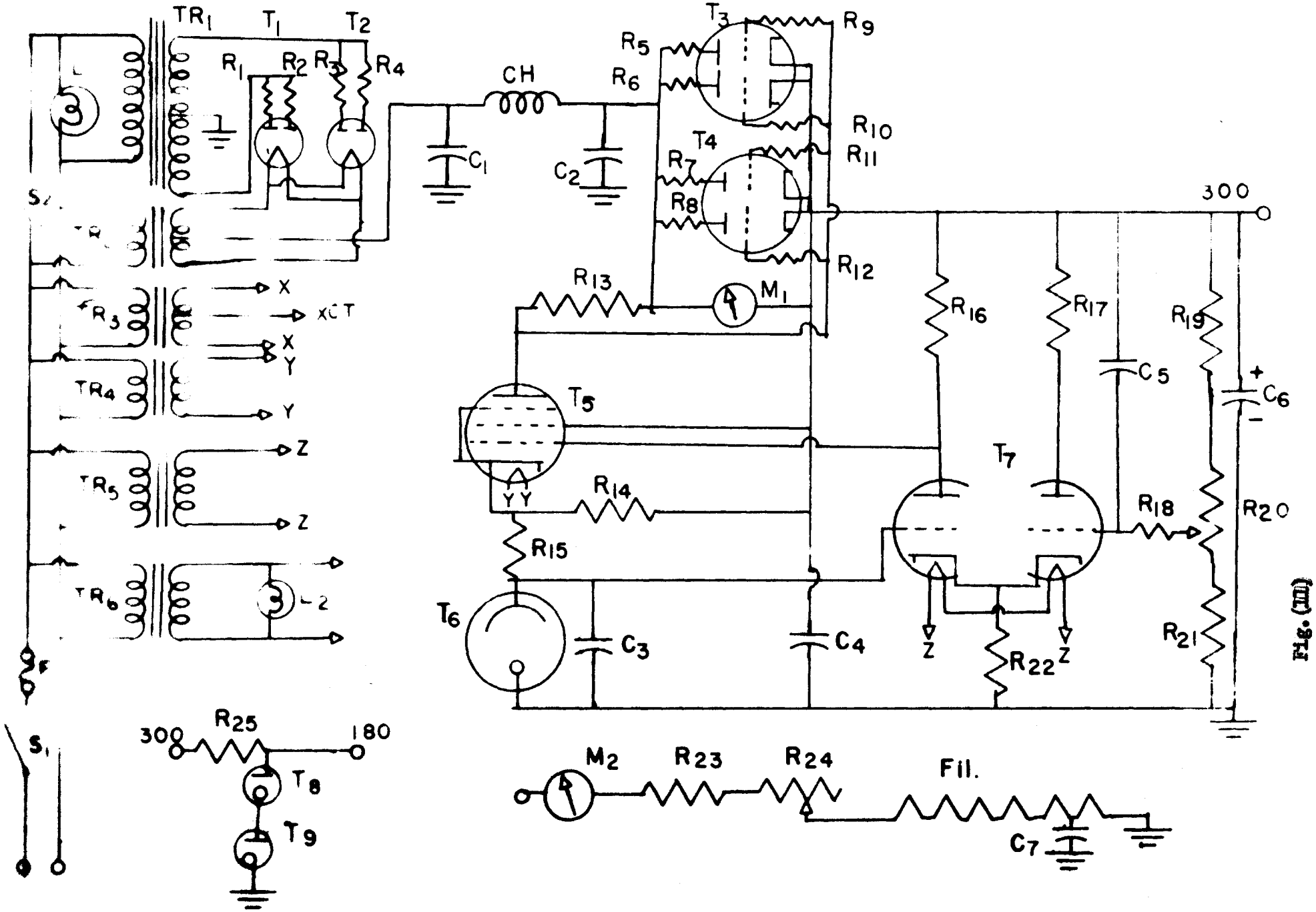
TR1
T1
T2
R1
R2
R3
R4
CH
C1
C2
T3
R5
R6
R9
R10
R11
T4
R7
R8
R12
300
R13
M1
R16
R17
R19
C5
C6
T5
T7
YY
R14
R18
R20
R15
T6
C3
C4
Z
R22
R21
X
XCT
X
Y
Y
Z
Z
TR3
TR4
TR5
TR6
L2
S1
R25
300
180
T8
T9
M2
R23
R24
Fil.
C7

Fig. (III)

before being sent to the phase-sensitive detector. The other detector T5 forms part of an automatic volume control circuit and is coupled through a filter circuit to the normally grouded grid of the oscillator tube T1. The filteres d.c. signal from this detector is proportional to the r.f. level, and because of the a.v.c. (T5), the r.f. level is maintained at a constant predetermined value as the frequency is varied.

(b) Power Supply for Oscillating Detector

Since the oscillating detector is operated at very low levels of oscillation, it is very sensitive to any stray oscillating electric or magnetic fields and to changes in the supply voltage. It is essential, therefore, to have an extremely well stabilized power supply. Also the filaments of the tubes should be operated on d.c. current to burther minimize stray pick-up. Batteries were tried at first for the filaments but they proved unsatisfactory, because first, the large current drain necissitated frequent recharging, and second, the potential of the batteries kept changing causing the r.f. level to drift.

The power supply shown in figure(11) makes use of a 6SL7(T_7) as a difference amplifier. This type of amplifier is used because if the current through both halves of the tube are equal, the variation of amplification due to a change in filament temperature is negligible

The reference voltage is supplied by a VR 105 (T_6) which has the best characteristics of the VR series. The current for the VR105 is taken from the stabilized side of the power supply to ensure stable

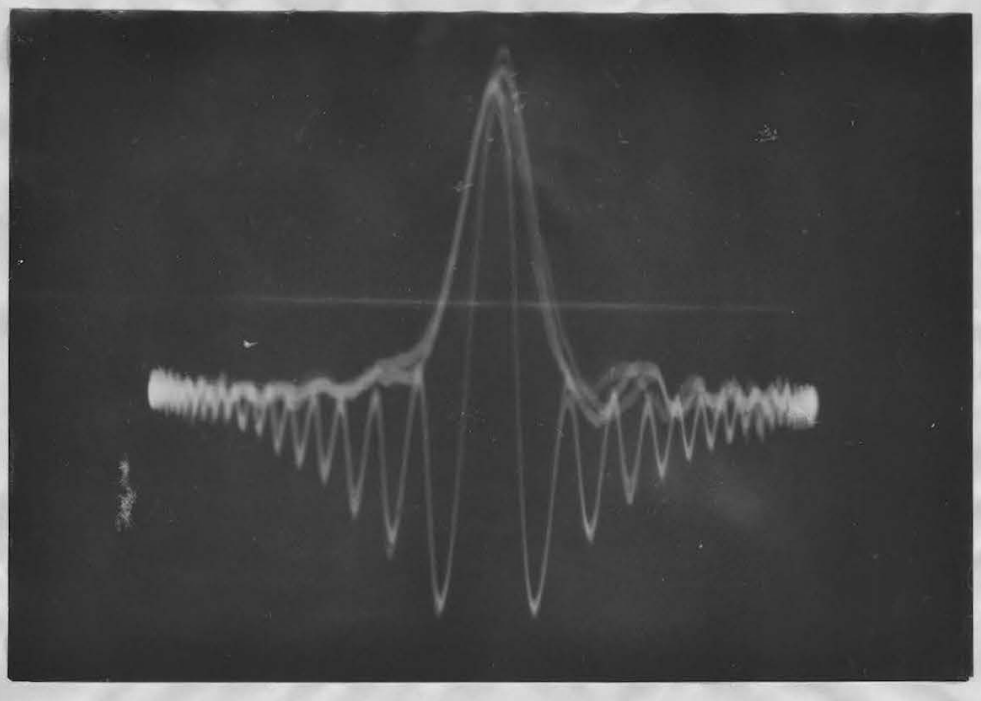

Fig (12) A proton signal in mineral oil photographed from an oscilloscope screen.

operation. Since the VR tubes have high a.c. resistance, a 0.1 mfd condenser is connected in parallel with it to bypass the a.c..

The power is supplied by a full wave rectifier using two 5U4 rectifier tubes (T1 and T2), smothed in a π filter and controlled by two 6AS7 tubes(T3 and T4) in parallel. The doubling of the tubes is necessary because of the large current to be supplied, 150 ma for the filaments of the oscillating detector. This current is obtained from the 300 volt supply by dropping the voltage across two 750 ohm 100 watt resistors(R_{23} and R_{24}). 50 ma for the oscillating detector and 75 ma for the phase sensitive detector.

(5)(a) Magnetic Field Modulation

Since the resonance signals are of the same order of magnitude as the noise, everything possible must be done to make the signal obvious. If one simply varied the frequency through the resonance condition one would have to detect a single very small change in the r.f. level. It would be very difficult to pick out this one particular small change in the r.f. level from the random changes due to the noise. However, if one were to sweep back and forth at a constant audio frequency through the resonance condition, it would be relatively simple to pick out the signal, which would be repetitive at a known frequency, from the random noise. Also this technique has several practical advantages. First, the nuclear resonance signal will now appear as an audio modulation on an r.f. carrier so that standard radio circuit can be used to handle the signal, Second, after the detector stage a narrow band audio amplifier can be used which greatly

improves the signal to noise ratio

The resonence condition can be made repetitive by modulating the magnetic field. In the spectrometer described in this thesis the magnetic field is modulated by the magnetic field produced by an a.c. current passing through Helmholtz coils. These coils are mounted with their axis parallel to the static magnetic lines of force rpoduced by the electromagnet. The r.f. coil of the oscillating detector is placed at the geometrical center of the Helmholtz coils.

If the nuclear resonance signal is strong and relatively narrow it can be observed directly on the oscilloscope. This is usually done by modulating the magnetic field sinusoidally at a frequency of 60cycles/sec and at an amplitude several times the width of the nuclear resonance signal. The horizontal sweep of the oscilloscope is driven by the same signal that modulates the magnetic field. As an example, a proton signal from mineral oil with the conditions described above is shown in figure (12). Note that the signal is doubled because the oscilloscope plots the signal on both the backward and forward sweep. The wiggles have been explained by Jacobson and Wangness (16).

If it is desired that the signal should be automatically plotted on a recorder a different procedure must be used because ordinary recorders have too large an inertia to respond to an audio signal with a frequency of 60cycles/sec. This procedure to be described below, has the additional advantage that it results in a very narrow bandwidth so that the signal to noise ratio is much better. Thus weak signals that cannot be observed at all on the

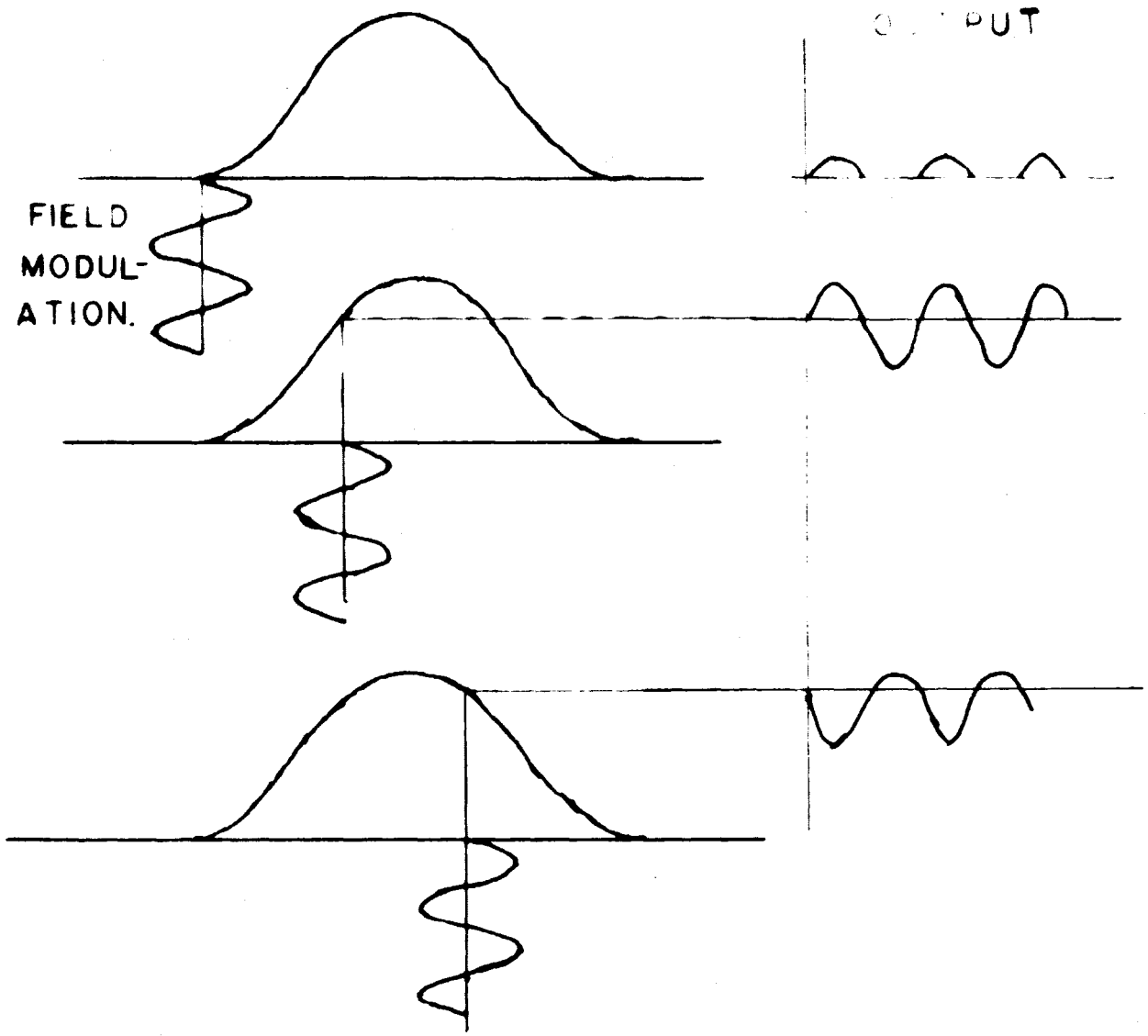

Fig.(13)

oscilloscope will appear very clearly on the recorder chart. In this method the modulation amplitide on the magnetic field is reduced to less than half the width of the nuclear resonance signal to be recorded and the frequency of the oscillating detector is slowly varied through the resonance condition. As the frequency of the oscillating detector is driven through the resonance condition the r.f. output from the oscillator is modulated, at the audio frequency of the magnetic field modulation, with an amplitude nearly proportional to the slope of the absorption curve. This can easily be understood by examining the diagrams in figure (13). The first two diagram illustrate the modulation effect on the slope of the absorption peak, the signal increasing in amplitude from zero to a maximum at the inflection point on the curve and decreasing to zero at the peak of the curve. The third diagram illustrates what happens when the peak is passed, it changes phase.

Before it can be plotted on the recorder this a.c. signal must be converted to a d.c. signal. This is accomplished by the phase-sensitive detector which not only converts the a.c. to a d.c. signal but also preserves changes in phase. If the modulation amplitude is not too large the output from the phase-sensitive detector is to a first approximation proportional to the first derivative of the absorption curve. The output from the phase-sensitive detector is filtered and then plotted on an Esterline-Angus recorder. An e xample of signals recorded in this way is shown in figure (14)

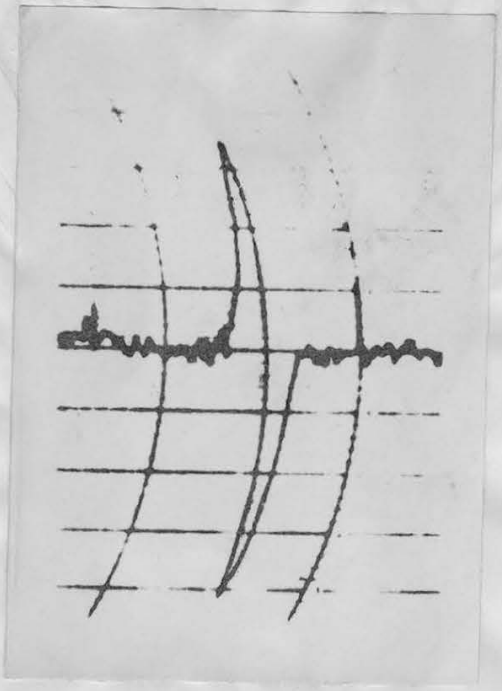

Fig.(14) Section of recorder chart showing an absorption peak

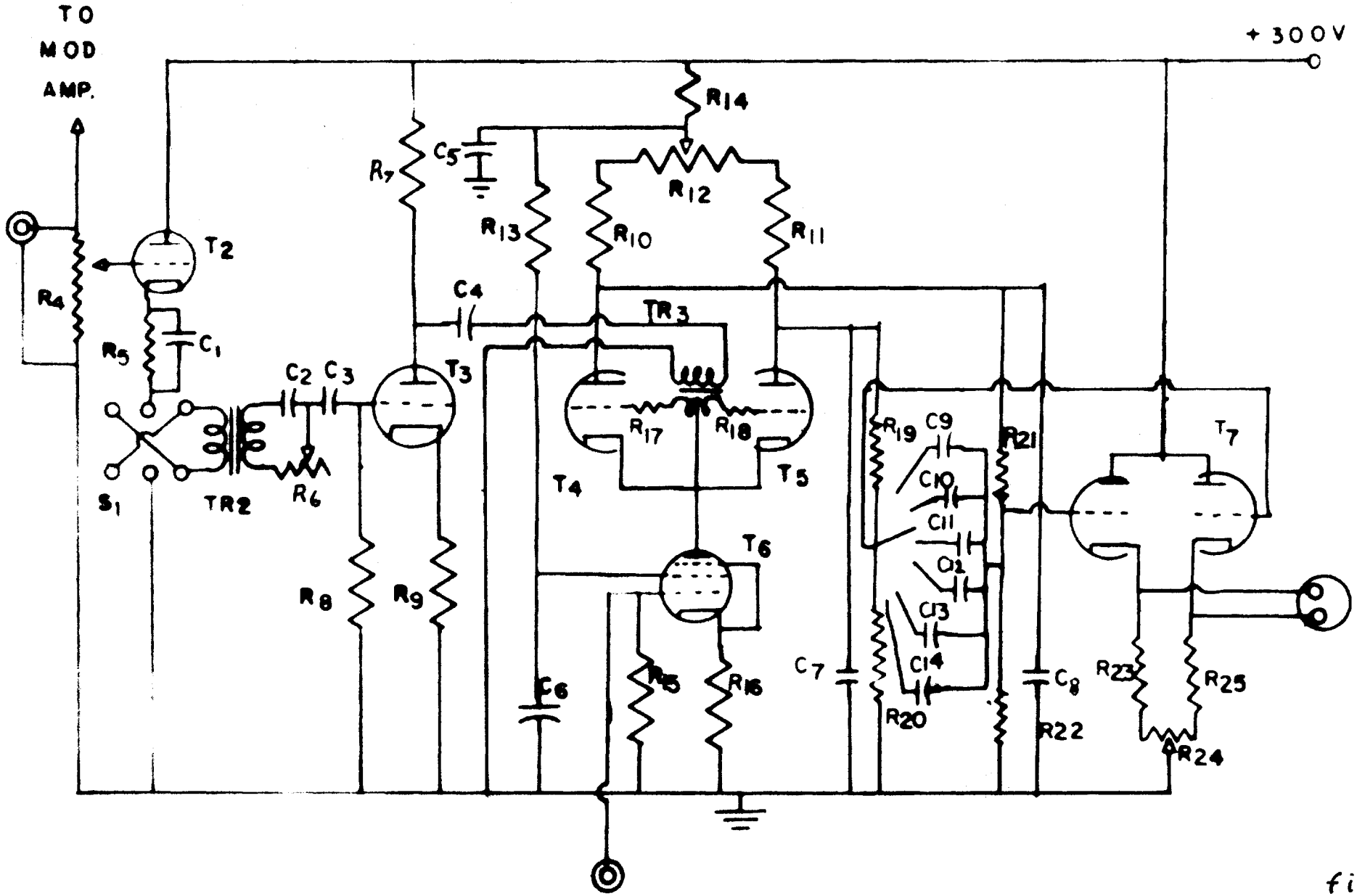
TO
MOD
AMP.
+300V
R14
R7
C5
R12
R13
R10
R11
T2
R4
C4
TR3
R5
C1
C2
C3
T3
T7
R19
C9
R21
R17
R18
T4
T5
C10
C11
T6
C12
C13
C14
R8
R9
C7
C8
R23
R25
C6
R15
R16
R20
R22
R24
S1
TR2
R6

fig 15

(5)(b) Phase-Sensitive Detector

The phase-sensitive detector shown in figure (15) is based on a design by N.A.Shuster (17). The circuit works as follows. The reference signal from the audio oscillator, a Hewlett-Packard type 200 AB Audio Oscillator, is fed through a cathode follower T_2, a phase shift network and an amplifier T3 to the grids of the 6SN7 double triode T4 and T5. The reference signals appearing at the grids of the triodes T4 and T5 are 180° out of phase and large enough to cut them off alternately. The grid resistors limit the grid potential to a small positive value relative to the cathode. The plate resistance of each section of the 6SN7 is about 7,000 ohms and small compared to the 1 megohm value for the 6SH7 T6 and may therefore be neglected. The double triode is therefore, just a switch. The signal plus noise from the oscillating detector comes onto the grid of the 6SH7. The switching action of the double triode rectifies the a.c. signals to provide a d.c. output which is plotted on a recording milliameter. When the output changes phase at the peak of the absorption signal (figure (13)) the polarity of the d.c. output from the switch reverses. The random noise is not rectified and due to the long time constant of the R.C. circuit following much of it is averaged out. The cathode followers are necessary to drive the pen of the recording milliameter because of the high resistance of R_{19}, R_{20}, R_{21}, and R_{22}.

This phase-sensitive detector possesses certain advantages over other types of circuits used. In others the switching frequency is

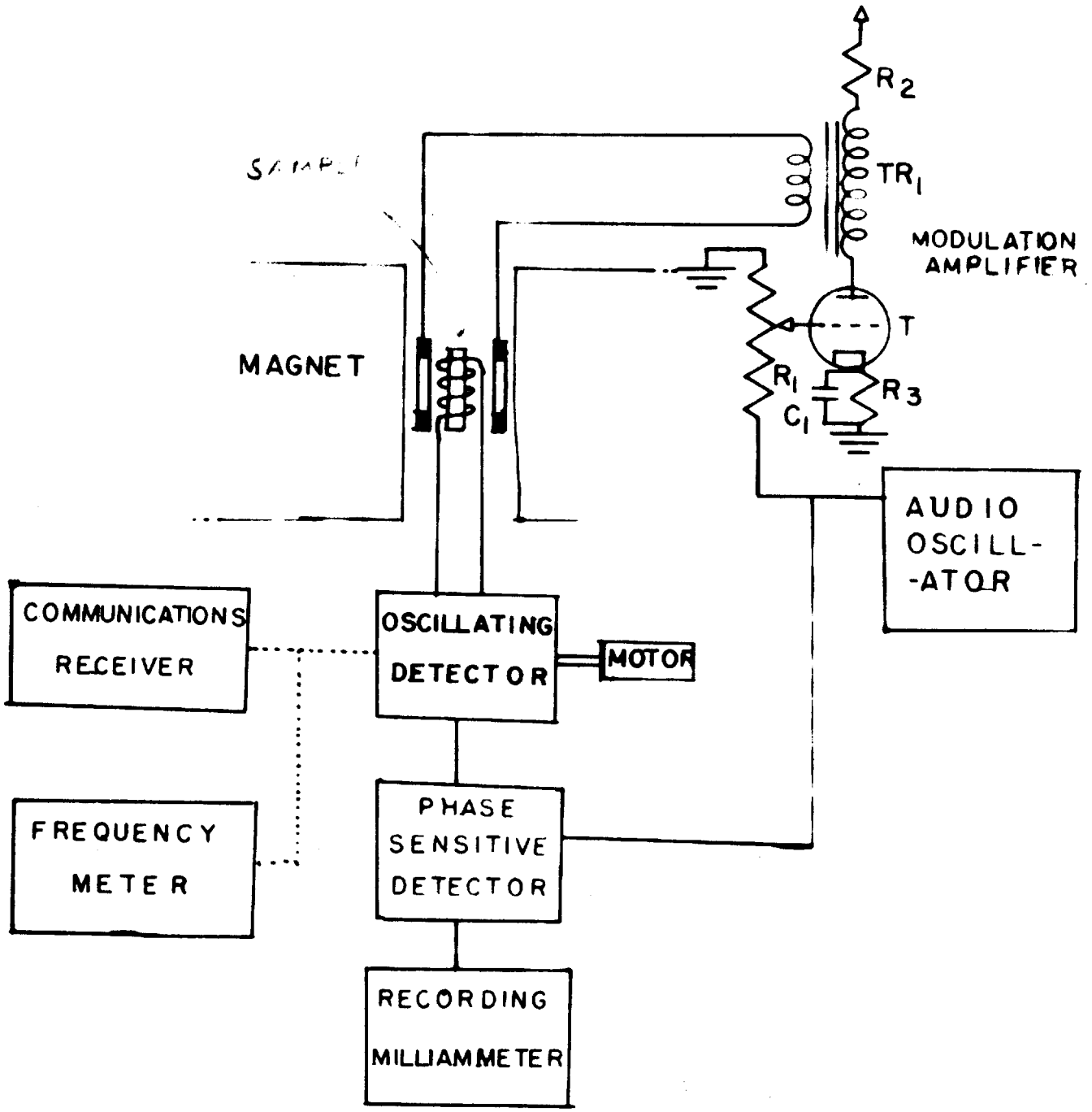
SAMPLE
MAGNET
R_2
TR_1
MODULATION AMPLIFIER
T
R_1
C_1
R_3
AUDIO OSCILL-ATOR
COMMUNICATIONS RECEIVER
OSCILLATING DETECTOR
MOTOR
FREQUENCY METER
PHASE SENSITIVE DETECTOR
RECORDING MILLIAMMETER

mixed with the signal plus noise giving interference. In this type the switching signal is in its own closed loop and cannot possibly interfere with the weak resonance signals. The signal is fed into a balanced circuit so that any variation of the tube parameters will cause little effect on the output. The only resistors which would have any effect on the balance of the circuit due to temperature changes are R_{10}, R_{11}, and R_{12}. R_{10} and R_{11} are precision wire-wound and R_{12} is a wire-wound potentiometer.

(6) Nuclear Magnetic Resonance Spectrometer.

Figure (16) shows the complete nuclear magnetic resonance spectrometer. The modulating coils are fed from the audio oscillator through an amplifier. The communications receiver is not attached to the oscillating detector and the frequency meter but picks up the r.f. transmitted by these two instruments and combines them to give the beat note.

Figure (17) is a photograph of the oscillating detector. One of the Helmholtz coils has been removed from the detector head to show the tank coil of the oscillator.

Figure (18) is a photograph of the apparatus. The oscillating detector is hidden behind the magnet on the right of the picture and the snychronous motor and gear train in the center. The audio oscillator. amplifier, phase-sensitive detector and power supply are in the rack in the center of the picture and the frequency, oscilloscope and recording milliameter in the rack on the left of the picture.

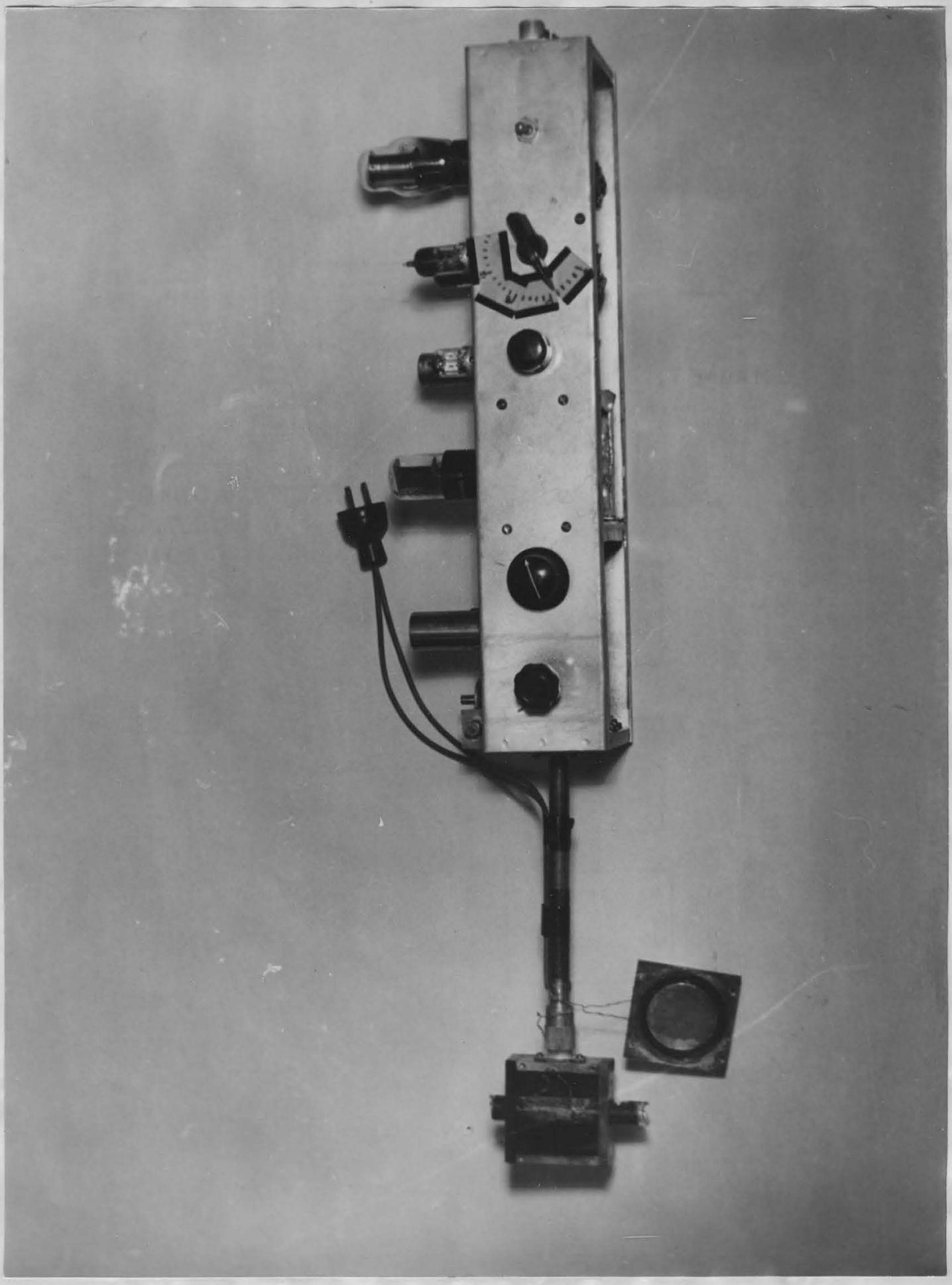

Fig. (17)

Fig. (18)

Parts list figure (3)

C_1 C_2	2 4mfd 3000 volt oil filled.
CH_1	Hammond 20V500 choke
F	5 amp 250 volt fuse.
L_1 L_2	6watt 120 volt lamp
S1 S_2	SPST toggle switch.
T_1 T_2	866-A/866 mercury vapor rectifier.
TR_1	General Radio type 200C Variac.
TR_2	Hammond Plate Transformer
	Primary 125-115-90-0 volts
	Secondary 1500-1250-0 volts 500 ma.
TR_3	Hammond high voltage transformer 1166X60.
CH_2	Hammond 10V500 choke.

Parts list figure (5)

C_1	·1 mfd paper	$R_{13}R_{14}R_{15}$	33 Kohm 1 watt
C2	·001 mfd paper	R_{16}	2·2 Kohm 1 watt
C_3	8 mfd electrolytic	$R_{17}R_{18}$	1 Megohm ½ watt
C_4	·001 mfd paper	R_{19}	1·5 Megohm ½ watt
C_5	8 mfd electrolytic	R_{20}	50 Kohm 10 watt
C_6 C_7 C_8 C_9	16 mfe electrolytic	R_{21}	75 Kohm 10 watt
$C_{10}C_{11}C_{12}$	·1 mfd paper.	R_{22}	6 Kohm 10 watt
C_{13}	·5 mfd paper	R_{23}	3 Kohm 10 watt
$C_{14}C_{15}C_{16}C_{17}$	100 mfd electrolytic	R_{24}	1 Kohm 10 watt
M	1-0-1 ma meter	R_{25}	10 Kohm potentiometer w.w.
R_1	40 ohm 10 watt	S	DPST toggle switch
R_2	10 Kohm w.w. "Helipot"	T_1 T_2 T_3	12SH7
R_3	47 Kohm ½watt	T_4	12J5
R_4 R_5 R_6 R_7	1 Megohm potentiometer	V_1 V_2	chopper
R_8	33 Kohm 2watt Ohmite		(Leeds and Notthrup.)
R_9 R_{10}	22 Kohm ½ watt		
$R_{11}R_{12}$	1 Megohm 1 watt		

Parts list (figure ()

C_1	1 mfd paper
C_2	16 mfd 450 volt electrolytic.
C_3	10 mfd 25 volt electrolytic.
C_4	0·1 mfd paper.
C_5	0·5 mfd paper.
C_6	25 mfd 25 volt electrolytic.
C_7	0·1 mfd paper.
R_1	1 Megohm 1 watt
R_2	470 Kohm 1 watt.
R_3	10 Kohm 1 watt.
R_4	100 Kohm 1 watt.
R_5	1·8 Kohm 1 watt.
R_6	1 Megohm linear potentiometer, carbon.
R_7	47 Kohm 1 watt.
R_8	1·8 Kohm 1 watt.
T_1	12SJ7.
T_2	½ 12SL7.

Parts list figure (7)

M_1	0-500 ma meter
M_2	0-100 volts meter
M_3	0-300 volts meter
R_1 R_2 R_3	1 Megohm 1 watt
R_4 R_5 R_6	500 Kohm precision 1% w.w.
R_7 R_8 R_9	100 Kohm precision 1% w.w.
$R_{10}R_{11}$	100 Kohm 1 watt carbon.
R_{12}	100 Kohm General Radio potentiometer w.w.
$R_{13}R_{14}$	1000 ohm 1 watt
$R_{15}R_{16}$	100 ohm 10 watt w.w.
R_{17}	4500 ohm 400 watt Cenco potentiometer
S_1 S_2	SPDT toggle switch.
T_1 T_2 T_3	½ 12 SL7
T_4 T_5	12J5
T_6 T_7	6B4.

Parts List figure (8)

C_1	10 mfd 600 volt oil filled	R_{12}	500 Kohm 1 watt
C_2	20 mfd 600 volt oil filled	R_{13}	10 Kohm 1 watt
C_3	10 mfd 600 volt oil filled	R_{14}	500 Kohm 1 watt
C_4	16 mfd 450 volt electrolytic	R_{16}	500 Kohm 1 watt
C_5	0•1 mfd paper	R_{15}	15 Kohm 20 watt
CH_1	Hammond # 10-200	R_{17}	100 Kohm 10 watt w.w.
CH_2	Hammond # 158	R_{18}	50 Kohm potentiometer w.w.
F	5 amp 250 volt fuse	R_{19}	100 Kohm 10 watt w.w.
Fil_1	filaments of the adding circuit.	S	SPST toggle switch
		T_1 T_5	5U4G
Fil_2	filaments of D.C. amplifier	T_2	3 6B4 in parallel
L	6 watt 120 volt lamp	T_3	12SH7
M	0-200 ma meter	T_4 T_8	VR 150
R_1	500 Kohm 1 watt	T_6	6AG7
R_2	500 Kohm 1 watt	T_7	6SH7
R_3	100 Kohm 10watt w.w.	TR_1	Hammond special #20539
R_4	50 Kohm potentiometer w.w.		Primary 115volts 170watts
R_5	100 Kohm 10watt w.w.		25 cycles
R_6	100 Kohm 10 watts w.w.		Secondary 5volts 3amps
R_7	50 Kohm potentiometer w.w.		6•3volts 2amps
R_8	100 Kohm 10 watts w.w.		6•3volts 4amps
R_9	15 Kohm 20 watts		400-0-0-400 volts 200 ma
$R_{10}R_{11}$	750 ohm 100 watts w.w.	TR_2	Hammond 275X60

Parts list figure (10)

C_1 0-250 mmfd variable condensor

C_2 C_3 0.01 mfd paper

C_4 2 mfd metallized

C_5 8 mfd electrolytic

C_6 50 mfd 25 VDC electrolytic

C_7 C_8 0.01 mfd paper

C_9 C_{10} C_{11} C_{12} 0.01 mfd paper

C_{13} C_{14} 0.001 mfd mica

C_{15} C_{16} C_{17} 0.01 mfd paper

C_{18} 2 mfd + 0.01 mfd paper

C_{19} 0.1 mfd paper

C_{20} 0.001 mfd mica

C_{21} 0.25 mfd paper

C_{22} 50 mfd 25VDC electrolytic

C_{23} 8 mfd electrolytic

L_1 L_3 L_4 r.f. peaking coil
30 turns #26 BandS wound on
Bakelite rods.

L_2 Ohmite Z-14 r.f. choke

R_1 1000 ohm 1 watt

R_2 3 Kohm 1 watt

R_3 R_4 R_5 2 Kohm 1 watt

R_6 3 Kohm 1 watt

R_7 R_8 5 Kohm 1 watt

R_9 10 Kohm 1 watt

R_{10} 25 ohm 1 watt

R_{11} 3.3 Kohm 1 watt

R_{12} 150 ohm 1 watt

R_{13} 300 ohm 1 watt

R_{14} 500 ohm potentiometer w.w.

R_{15} 1250 ohm 10 watt w.w.

R_{16} 25 ohm 1 watt

R_{17} 1000 ohm 1 watt

R_{18} 180 ohm 1 watt

R_{19} 20 Kohm 1 watt

R_{20} 180 ohm 1 watt

R_{21} 860 ohm 1 watt

R_{22} 470 ohm 1 watt

R_{23} R_{24} 470 Kohm 1 watt

R_{25} 1000 ohm potentiometer w.w.

R_{26} 33 Kohm 10 watt w.w.

R_{27} 3 Kohm 1 watt

R_{28} 22 Kohm 1 watt

R_{29} 100 Kohm 1 watt

R_{30} 10 Kohm 1 watt

R_{31} 56 Kohm 1 watt

R_{32} 22 K ohm 1 watt

R_{33} 0.1 Megohm potentiometer

Parts list figure (10)(cont.)

$R_{34}R_{36}$	4.7 Kohm 1 watt
$R_{35}R_{38}$	47 Kohm 1 watt
R_{37}	250 Kohm 1 watt
S_1	Mallory 11 point rotary switch
S_2	DPST toggle switch
T_1	12AU7
T_2	VR 150
T_3 T_4 T_6 T_8	12AW6
T_5 T_6	½ 12AL5

Parts list figure (11)

C_1	4 mfd 600 volts oil.
C_2	30 mfd 600 volts oil.
C_3 C_4 C_5	0.1 mfd paper
C_6	8 mfd electrolytic.
CH	Hammond 10X300 choke
F	5 amp 250 volt fuse
L_1	6 watt 120 volt lamp.
L_2	6 volt lamp
M_1	0-300 volt meter
M_2	0-300 ma meter.
R_1 R_2 R_3 R_4	100 ohm 10 watt w.w.
R_5 R_6 R_7 R_8	100 ohm 10 watt w.w.
R_9 R_{10} R_{11} R_{12}	1000 ohm 1 watt
R_{13}	500 Kohm 1 watt
R_{14}	10 Kohm 10watt w.w.
R_{15}	15 Kohm 10 watt w.w.
R_{16} R_{17} R_{18}	500 Kohm 1 watt
R_{19}	200 Kohm precision 1% w.w.
R_{20}	10 Kohm potentiometer w.w.
R_{21}	100 Kohm precision 1% w.w.
R_{22}	2.25 Kohm 1 watt
R_{23} R_{24}	750 ohm 100 watt w.w.
R_{25}	5 Kohm 20 watt w.w.
T_1 T_2	5U4
T_3 T_4	6AS7
T_5	6SJ7
T_6	VR 105
T_7	6SL7
T_8	VR 105
T_9	VR 75
TR_1	Hammond power transformer #715
TR_2	Hammond transformer #165
TR_3	" " #112S
TR_4	" " #167B
TR_5	" " #167B
TR_6	" " #167E

Parts list figure (15)(16)

C_1	25 mfd 25 volt electrolytic	R_{15}	330 Kohm potentiometerw.w.
C_2	0.01 mfd paper	R_{16}	800 ohm 1 watt
C_3	0.05 mfd paper	$R_{17}R_{18}$	220 Kohm 1 watt
C_4	2 mfd paper	$R_{19}R_{20}R_{21}R_{22}$	470 Kohm 1 watt
C_5	8 mfd electrolytic	$R_{23}R_{24}$	5 Kohm 20 watt w.w.
C_6	40 mfd electrolytic	R_{25}	General Radio potentiometer
C_7 C_8	2 mfd paper		20 Kohm w.w.
C_9	0.1 mfd paper	S_1	DPDT toggle switch
C_{10}	0.25 mfd paper	S_2	Mallory 6 point switch
C_{11}	0.5 mfd paper	T_1	6V6
C_{12}	1 mfd paper	T_2	6J5
C_{13}	2 mfd paper	T_3	6C4
C_{14}	8 mfd oil	T_4	6SN7
R_1 R_4	1 Megohm linear pot.	T_5	6SN7
R_2	4.5 Kohm 10 watt w.w.	T6	6SH7
R_3	270 ohm 1 watt	T7	6SN7
R_5	1.5 Kohm 1 watt	TR_1	Hammond transformer #1618
R_6	250 Kohm potentiometer	TR_2	Hammond transformer #333
R_7	47 Kohm 1 watt	TR_3	Hammond transformer #933
R_8	470 Kohm 1 watt		
R_9	1.5 Kohm 1 watt		
$R_{10}R_{11}$	50 Kohm precision w.w.		
R_{12}	20 Kohm 1 watt		
R_{13}	50 Kohm 1 watt		
R_{14}	5 Kohm 1 watt		

Experimental Procedure

The procedure to be followed when using this spectrometer to measure the nuclear magnetic resonance absorption spectrum in a crystal can be described briefly. The crystal, fastened to a mount, is suspended in the tank coil of the oscillating detector. This tank coil figure (10) it will be remembered, is mounted in the gap of the electromagnet. The magnet power supply and other electronic equipment is turned on and given time to warm up to its operating temperature. The approximate frequency at which the signals will be found for a particular nuclear species can be quickly calculated by using equation (18) with the value of the field strength obtained from the calibration curve figure (9), and the value for the magnetic moment and spin for the nucleus in question. The magnetic moments and spin for various nuclear species are available in several tables such as that by Mack(18).

The tuning condenser in the oscillating detector is adjusted so that the oscillation frequency is higher than the calculated resonance frequency. The frequency of the oscillating detector is then slowly driven through the interesting region by means of a synchronous motor coupled to the variable condenser by a train of reduction gears. Frequency markers are made at intervals on the chart so that by interpolation one can obtain the frequency of any signals that appear.

Frequency measurements are made by simultaneously picking up the unknown frequency and a known frequency on a Hallicrafters type

SX-62A receiver and then adjusting the known frequency to give zero beat. A General Radio type 620-A Heterodyne frequency meter is used to produce the known frequency.

Some of the results to be described later were obtained with the crystal at various temperatures. A stream of cold gas, produced by boiling liquid oxygen in a three litre dewar flask, was used to cool the crystal. The cold oxygen passed through a heat-insulated glass tube, held in place by a styrofoam stopper in the neck of the vacuum flask, and then flowed over the crystal. The rate of boiling was controlled by the current through a small immersion heater consisting of a coil of nichrome wire. Temperatures as low as -100°C were easily obtained in this manner.

The high temperature results were obtained by suspending the crystal in a hot oil bath. A 100 ml. flask was prepared by winding a coil with thirty turns of copper wire on its neck and several turns of nichrome wire, to be used as a heater around its base. The entire flask was then covered with asbestos for heat insulation and to hold the two coils in place. The flask, partially filled with melting-point oil, was then mounted so that its neck, with the thirty turn coil, occupied the region in the magnetic field normally occupied by the tank coil of the oscillating detector. In this case the coil on the neck of the flask was used as the tank coil. The crystal was then lowered down the neck of the flask until, immersed in the hot oil, it was located in the center of the tank coil. The temperature was controlled by the current through the nichrome heater. Temperatures as high as 300°C were obtained in this

manner.

The temperature of the crystals was measured in each case with a copper-constantan thermocouple and a Leeds and Northrup potentiometer.

Experimental Results and Discussion

Some experimental results have been obtained, although the major part of this thesis has to do with the construction of the nuclear magnetic resonance spectrometer which has already been described.

The spectrometer was tested by observing signals in liquid and in two crystals, spodumene and sapphire, which have already been examined by other workers. The electric quadrupole splitting of the Al^{27} signal in sapphire has been studied as a function of temperature and the results are given in this thesis. In addition, at the request of Dr. H. E. Petch a brief search was made for the B^{11} and Na^{23} signals in colemanite and sodium dihydrogen phosphate respectively.

In liquid samples, signals from the following nuclei have been observed on the oscilloscope: H^1, Li^7, Al^{27}, and F^{19} in water and mineral oil, aqueous solution of LiCl, aqueous solution of $AlCl_3$, and fluorobenzene respectively. The signals from solid samples are usually too small to be observed on the oscilloscope, but for one orientation of a large crystal of spodumene a signal from Li^7 was clearly observed. Signals from Li^7, Al^{27}, Na^{23} and B^{11} in single crystals of spodumene, artificial sapphire, sodium dihydrogen phosphate, and colemanite respectively have been recorded.

Spodumene, sapphire, sodium dihydrogen phosphate and colemanite are all non-isotropic so that one expects that there will be a non-vanishing electric field gradient at the nuclear sites. Therefore each nuclear resonance absorption signal is likely to be split into its 2I components. The number of sets of 2I components will depend

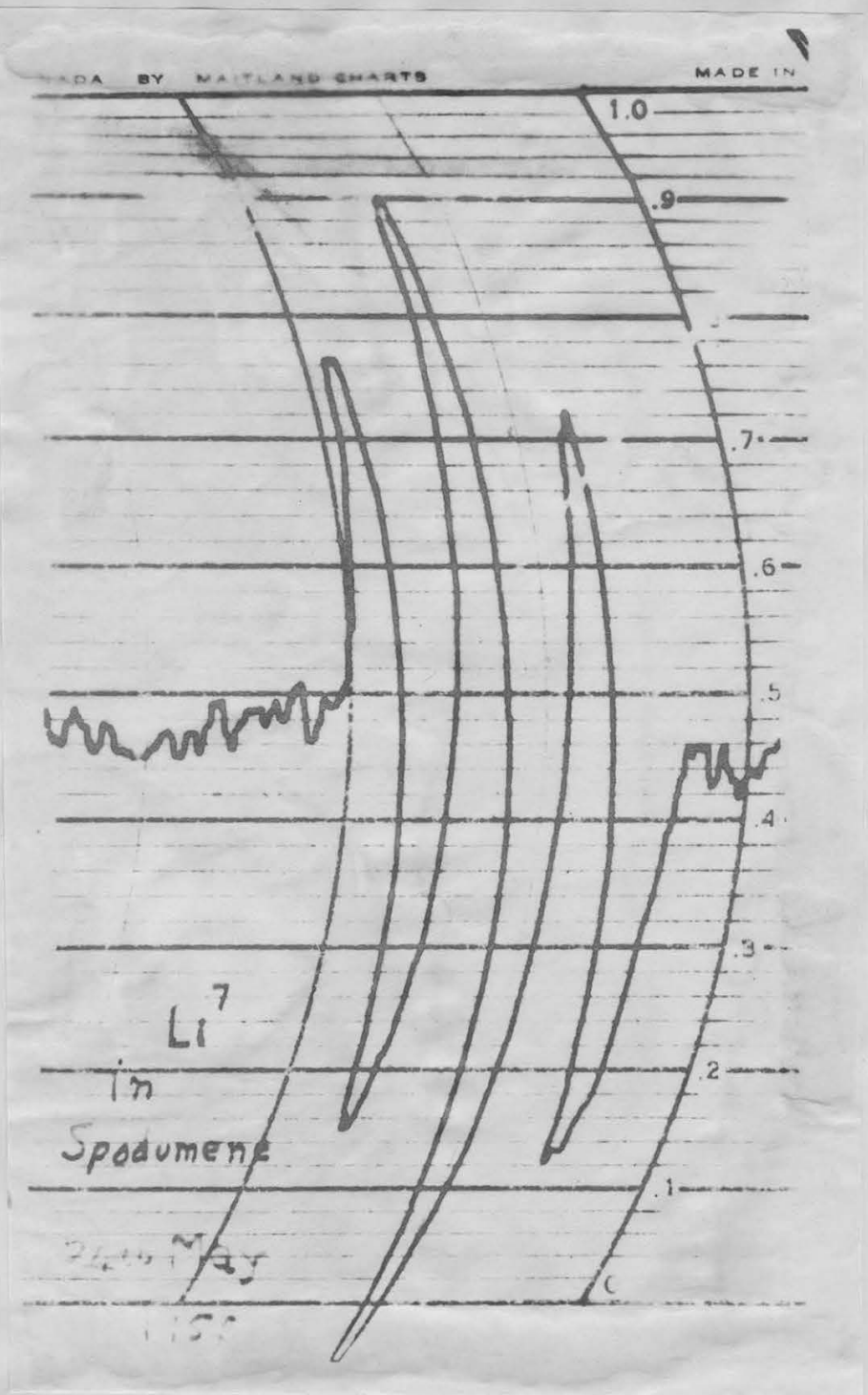

Fig, (20)

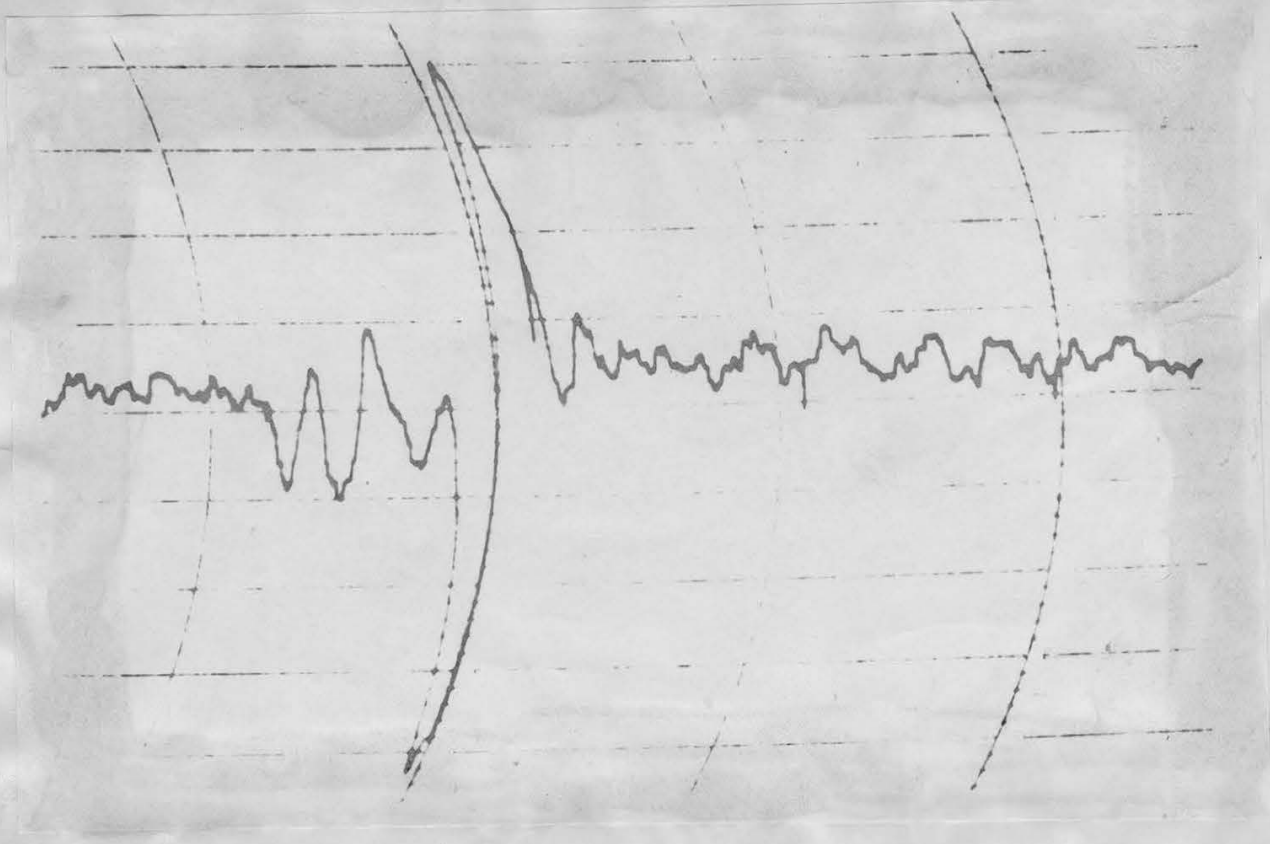

Fig. (21)

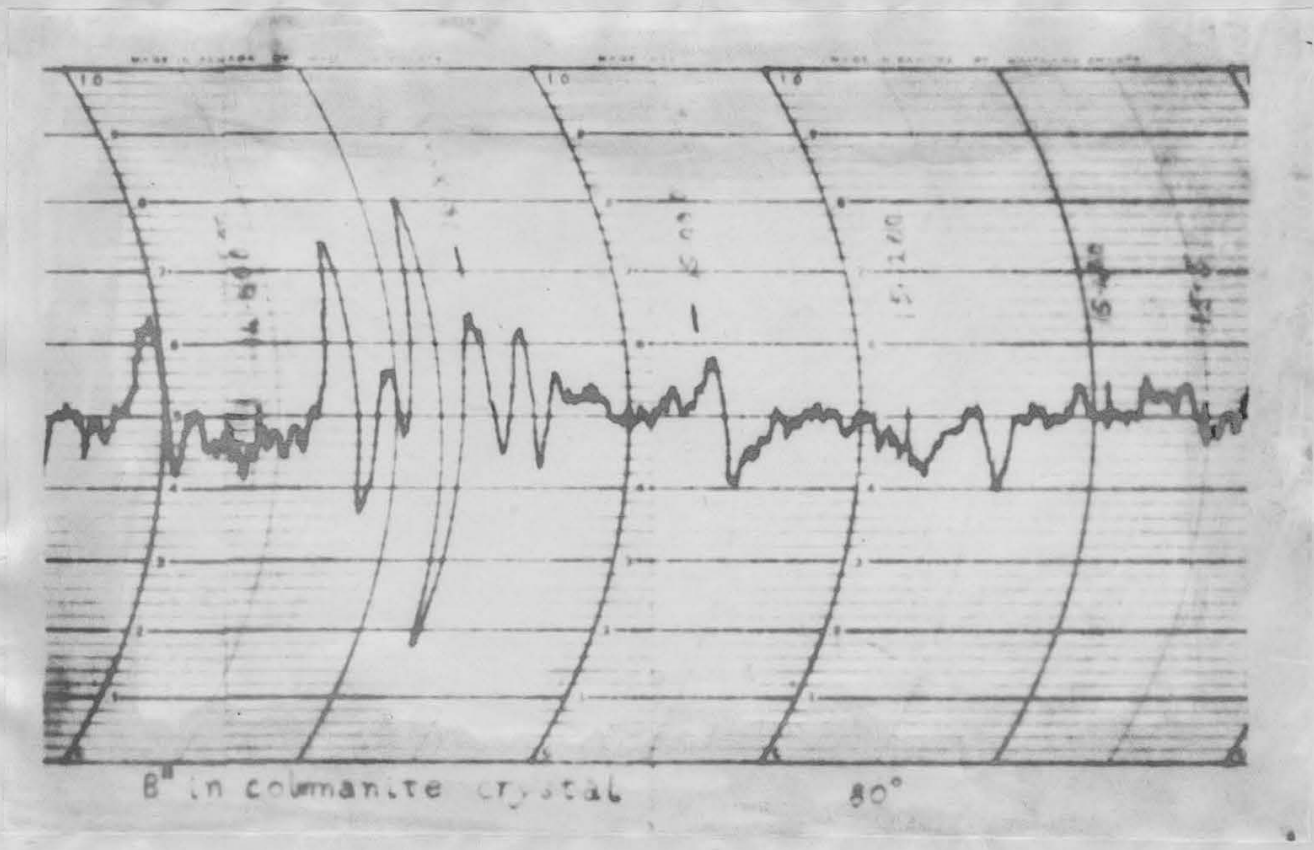

Fig. (22)

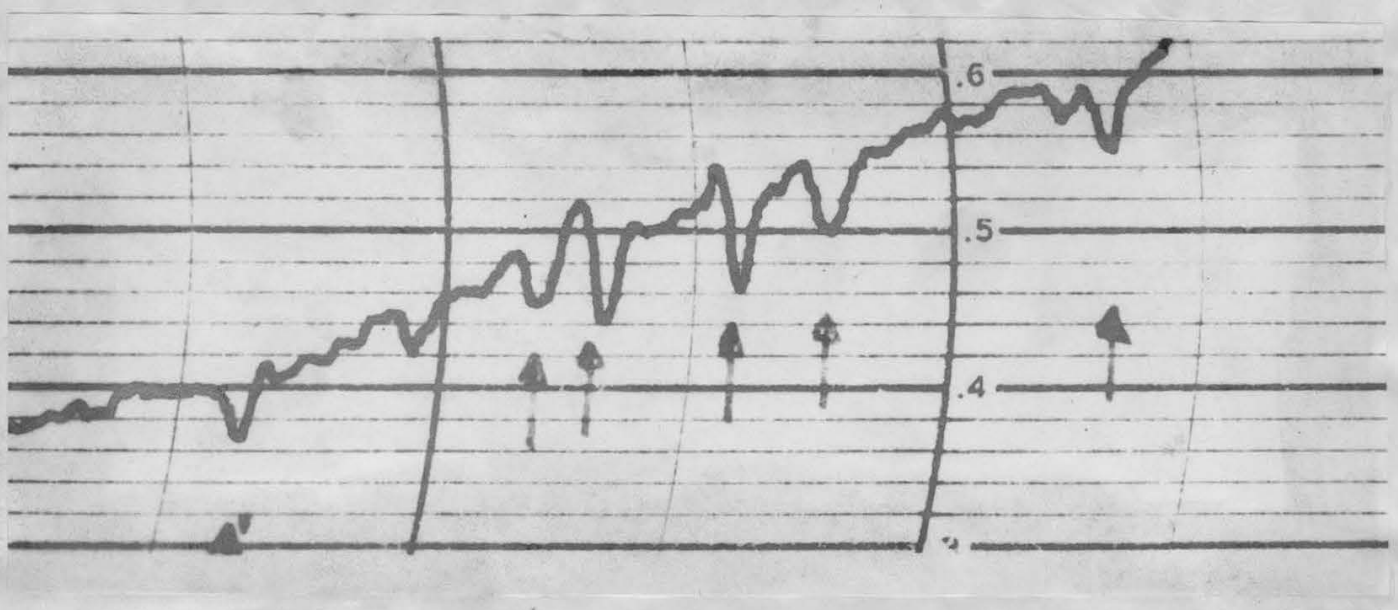

Fig.(23) Spectrum of Na^{23} in sodium dihydrogen phosphate.

on the number of non-equivalent positions that the nuclei of the type under consideration, occupy in the unit cell of the crystal. Single crystals are used so that the relative orientation with respect to the magnetic field will be the same for all sections of the crystal.

The spin of Al^{27} is 5/2 so that there are $2I=5$ possible transitions between the energy levels available to any one nucleus. Therefore five lines should appear for each non-equivalent Al site in the unit cell Al_2O_3. Since only five lines were found all the Al sites in Al_2O_3 must be equivalent. Similarly all the Li^7 sites in the unit cell of the spodumene crystal must be equivalent because only three signals due to Li^7 ($I=3/2$) were found. These are not new results but have been included since they show one of the uses of a nuclear magnetic resonance spectrometer. Figure (20) shows a signal obtained from a spodumene crystal showing the three resonance signals due to Li^7 just barely resolved.

A very complex spectrum was found in colemanite. Figures (21) and (22) show the B^{11} signals obtained in colemanite for two different orientations of the colemanite crystal. The crystal came from Death Valley, California. As many as six lines were observed but this probably does not represent the complete B^{11} spectrum.

A complex spectrum was also found for Na^{23} in $NaH_2PO_4 \cdot H_2O$ This is shown in figure (23). This crystal was grown from an aqueous solution by Mr. F. Holuj.

The complex spectra of B^{11} in colemanite and Na^{23} in sodium dihydrogen phosphate are extremely interesting and merit further work. The spins of B^{11} and Na^{23} are both 3/2 so there must be more than one

non-equivalent position for both boron and sodium in colemanite and sodium dihydrogen phosphate respectively since more than three lines were observed for each. A complete analysis of the spectra in each of these crystals will be needed to find out exactly the number of non-equivalent positions and the relative orientation of the principle axes for the electric field gradient at each site. Further work is being done on these two crystals by the Solid State group at McMaster University.

Change of the Degree of Ionicity as a Function of Temperature in the Al_2O_3 crystal

A convincing theory of ferroelectricity has been built by Megaw(19) around the assumption that the degree of ionicity of chemical bonds in crystals is a function of temperature. Now it has been shown by Townes and Daily(20) that the electric field gradient at a nuclear site is strongly dependent on whether the bonding is ionic or covalent in nature. They calculate that the electric field gradient at a nuclear site will be approximately a hundred time greater for covalent bonding than for ionic bonding. Therefore the electric quadrupole coupling constant for a given nucleus depends strongly on the type of bonding in which the atom, to which the nucleus belongs, is involved. Nuclear resonance determinations of the electric quadrupole coupling constants should be able to throw some light on whether Megaw's assumption is correct.

At one particular orientation, that gave a large splitting of the Al^{27} signal, the crystal was held fixed. Then the splitting

of the Al^{27} signal was measured while the crystal temperature was held at -100°C, 30°C and 300°C

The results are given in the following table;

Orientation	Temp.	Absorption peaks Mc/sec				
		2nd Sat.	1st Sat	Center	1st Sat'	2nd Sat'
I	30°C	6.575	6.335	6.115	5.875	5.759
	-100°C	6.575	6.336	6.115	5.878	5.758
II	30°C	6.585	6.341	6.117	5.916	
	30°C	6.618	6.343	6.117	5.920	5.749
	300°C	6.619	6.345	6.112	5.917	5.744
	300°C	6.590	6.340	6.116	5.916	

Magnetic Field 5,570 ± 1 gauss

In the experiment performed with the Al_2O_3, the crystal was held firmly in one orientation while the frequency of the Al^{27} components were measured at various temperatures. A change in the type of bonding would have resulted in a shifting of these frequencies. Within our limits of error (±5 kc/sec) no shifting was detected. Therefore any change in the degree of ionicity of the bonds in Al_2O_3 in the temperature interval -100°C to 300°C must be small. Because of instrumental difficulties these measurements were not made as accurately as they might have been. For this reason it is felt that the experiment should be repeated with more careful instrumentation and over a larger temperature range.

References

(1) H.Kopfermann Kernmomente Chapt.II Edward. Brothers Inc. Ann Arbor (1945)

(2) D.R.Hamilton. Am. J. Physics 9, 319, (1941)

(3) J.B.M.Kellogg and S.Millman. Rev. Mod. Physics 18, 323, (1946)

(4) Purcell Torrey and Pound. Phys, Rev. 69, 37, (1946)

(5) Bloemburgen, Purcell and Pound. Phys. Rev. 73, 679, (1948)

(6) Bloch, Hanson and Packard. Phys. Rev. 69, 127, (1946)

(7) F.Bloch. Phys. Rev. 70, 460, (1946)
Bloch, Hanson and Packard. Phys. Rev. 70, 474, (1946)

(8) G.E.Pake. J. Chem. Physics. 16, 327, (1948)

(9) Gutowski, Kistiakowski, Pake and Purcell. J. Chem. Physics 17, 972, (1942)

(10) N.L.Alpert. Phys. Rev. 75, 398, (1949)

(11) H.Gutowski and G.E.Pake J. Chem. Physics. 18, 162, (1950)

(12) Bethe H.A. Elementary Nuclear Theory John Wiley and Sons, Inc. New York.

(13) Rosenfeld. L. Nuclear forces p.64 Interscience Inc. New York

(14) R.V.Pound. Phys. Rev. 79, 685, (1950)

(15) R.V.Pound and W.D.Knight Rev. Sci. Inst. 21, 219, (1950)

(16) B.A.Jacobson and H.K.Wangness Phys. Rev. 73, 942, (1948)

(17) M.A.Shuster Rev. Sci. Inst. 22, 254, (1951)

(18) J.E.Mack Rev. Mod. Physics. 22, 64, (1950)

(19) H.D.Megaw. Acta. Cryst. 5. 739. (1952)

(20) C.H.Townes and B.P.Daily J. Chem. Physics. 17, 789, (1949) 20, 35 (1952)